Revisiting the ca. 845–820-Ma S-type granitic magmatism in the Jiangnan Orogen: new insights on the Neoproterozoic tectono-magmatic evolution of South China

Article *in* International Geology Review · February 2018

DOI: 10.1080/00206814.2018.1426054

International Geology Review

ISSN: 0020-6814 (Print) 1938-2839 (Online) Journal homepage: http://www.tandfonline.com/loi/tigr20

Revisiting the ca. 845–820-Ma S-type granitic magmatism in the Jiangnan Orogen: new insights on the Neoproterozoic tectono-magmatic evolution of South China

Teng Deng, Deru Xu, Guoxiang Chi, Yuhua Zhu, Zhilin Wang, Genwen Chen, Zenghua Li, Junling Zhang, Tingwei Ye & Deshui Yu

INTERNATIONAL GEOLOGY REVIEW, 2018
https://doi.org/10.1080/00206814.2018.1426054

ARTICLE

Revisiting the ca. 845–820-Ma S-type granitic magmatism in the Jiangnan Orogen: new insights on the Neoproterozoic tectono-magmatic evolution of South China

Teng Deng[a,b,c], Deru Xu[a,c], Guoxiang Chi[c], Yuhua Zhu[a,b], Zhilin Wang[d], Genwen Chen[a], Zenghua Li[c], Junling Zhang[a], Tingwei Ye[a,b] and Deshui Yu[a,b]

[a]Key Laboratory of Mineral and Metallogeny, Guangzhou Institute of Geochemistry, Chinese Academy of Sciences, Guangzhou, Guangzhou, China; [b]University of Chinese Academy of Sciences, Beijing China; [c]Department of Geology, University of Regina, Regina, Canada; [d]School of Geoscience and Info–Physics, Central South University, Changsha, China

ABSTRACT
The Neoproterozoic tectonic evolution of the Jiangnan Orogen is controversial, with one of the issues being whether the ca. 850–820-Ma granitoids were generated by mantle plumes or the collision between the Yangtze and Cathaysia blocks. This paper tackles this problem by examining the age and petrogenesis of one of the granitoids, the Getengling pluton in the central Jiangnan Orogen, and through comparison with a regional geochronological–geochemical database compiled from previous studies. The Getengling pluton is characterized by high A/CNK values (~1.5), slight negative whole-rock $\varepsilon_{Nd}(t)$ values (−2.8 to −3.4), and positive zircon $\varepsilon_{Hf}(t)$ values (0.7 ± 1.1), suggesting S-type granite affinities with juvenile contributions. Rb/Sr, Rb/Ba, and high CaO/Na_2O ratios indicate psammitic sources with both clay-rich and clay-poor characters. These geochemical characteristics are distinct from those of the granitoids (typically of A type) associated with mantle plumes. The zircon laser ablation-inductively coupled plasma-mass spectrometry U–Pb age of 845 ± 4 Ma obtained in this study, together with other ca. 835–820 Ma ages of S-type granites in the Jiangnan Orogen, indicates that the felsic magmatism in the Jiangnan Orogen lasted for ca. 25 Ma, which is longer than typical plume-related felsic magmatism. In addition, the mafic rocks in the Jiangnan Orogen and elsewhere in the South China Block are geochemically distinct from the coeval mantle plume-related ones in Australia and west Laurentia. In geochemical diagrams diagnostic of tectonic settings, the Getengling pluton and other ca. 850–820 Ma intrusions plot in the syn- and post-collisional fields, whereas the pre-850 and post-820-Ma igneous rocks plot in the arc and within-plate settings, respectively. This sequential tectonic evolution from plate subduction through collision to within-plate environments further supports the hypothesis that the ca. 850–820-Ma granitoids in the Jiangnan Orogen resulted from the Yangtze–Cathaysia collision rather than from mantle pluming.

ARTICLE HISTORY
Received 27 September 2017
Accepted 7 January 2018

KEYWORDS
Getengling pluton; S-type granite; Jiangnan Orogen; South China; northeastern Hunan Province; Neoproterozoic

1. Introduction

The Jiangnan Orogen, also called the Jiangnan Oldland, has been widely interpreted as the collisional belt between the Yangtze and Cathaysia blocks of the South China Block (Li *et al.* 2003a; Yao *et al.* 2013, 2014a; Wang *et al.* 2014; Xu *et al.* 2017). However, the timing and evolution of the orogeny are still debatable (Li 1999; Zhou *et al.* 2002; Zheng *et al.* 2008, 2008b; Zhao and Cawood 2012; Yao *et al.* 2014a, 2015b). One group of researchers suggested that the collision of the Yangtze and Cathaysia blocks happened at ca. 1100–900 Ma, associated with the global Grenville orogeny (Li *et al.* 1999, 2007b, 2008c; Ye *et al.* 2007; Yang *et al.* 2016; Lyu *et al.* 2017), whereas others considered that the assembly occurred at ca. 860–820 Ma (Zhou *et al.* 2009; Zhao and Cawood 2012; Yao *et al.* 2014a, 2015b).

Widespread Neoproterozoic felsic-dominated magmatism has been reported in the Jiangnan Orogen, including the ca. 1000–860-Ma I-type dominated, ca. 860–820-Ma S type, and ca. 820–730-Ma A- and S-type granites, as well as small amounts of mafic rocks (Li 2003; Li *et al.* 2003a; Gao *et al.* 2009; Wang *et al.* 2012c). In addition, there are several ca. 860–790 Ma bimodal volcanic rock intervals in the Neoproterozoic formations (Wang *et al.* 2008a; Wang *et al.* 2011b; Lyu *et al.* 2017). The controversy of the timing of Yangtze–Cathaysia collision arises from the different tectonic interpretations for the Neoproterozoic magmatic rocks.

CONTACT Deru Xu xuderu@gig.ac.cn Key Laboratory of Mineral and Metallogeny, Guangzhou Institute of Geochemistry, Chinese Academy of Sciences, Guangzhou, Guangzhou 510640, China
Supplemental data for this article can be accessed here.

According to the first model, the ca. pre-880-Ma metamorphic and magmatic events in the Jiangnan Orogen were generated by the collision between the Yangtze and Cathaysia blocks, while the post-860-Ma magmatic rocks including the bimodal volcanic rocks were generated under a rift setting in relation to mantle plume activities peaking at ca. 825 and ca. 780 Ma (Wang *et al*. 2008a, 2011b; Li *et al*. 2010b; Yang *et al*. 2016; Lyu *et al*. 2017). In contrast, the second model suggests that the 1000–860-Ma magmatic rocks with some having adakitic signatures were generated by plate subduction, whereas the ca. 860–820-Ma S-type granites, ophiolites, and other associated mafic–felsic rocks are related to collision between the Yangtze and Cathaysia blocks (Shu *et al*. 2006; Wang *et al*. 2006; Zhang *et al*. 2012b, 2013a; Cawood *et al*. 2017), and the post-820-Ma A- and S-type granites, bimodal volcanic rocks and other igneous rocks resulted from re-separation of the Yangtze and Cathaysia blocks after the first collision (Zhou *et al*. 2009; Zhao and Cawood 2012; Wang *et al*. 2012c; Yao *et al*. 2014a).

One of key differences between the two models is about the genesis of the ca. 835–820-Ma granitoids in the Jiangnan Orogen (Li *et al*. 2003a; Wang *et al*. 2006). The first model (referred to as the 'plume-rift model' hereinafter) interprets these granitoids to be formed by mantle plume activities under an anorogenic setting, which is consistent with the development of coeval bimodal volcanic rocks (Li *et al*. 2003a; Li *et al*. 2008c; Lyu *et al*. 2017). The second model (referred to as the 'slab-arc model' hereinafter), however, believes that these granitoids resulted from collision between the Yangtze and Cathaysia blocks, as supported by their S-type signatures (with certain I-type characteristics) (Wang *et al*. 2006; Zhao *et al*. 2011; Zhao and Cawood 2012). While acknowledging the geochemical characteristics of the granitoids are atypical of those associated with mantle plume activity (typically of A type), the 'plume-rift model' argued that tectonic interpretations based on geochemical discrimination diagrams are unreliable due to modification by mixed sources (Li *et al*. 2003a, 2006; Wang *et al*. 2010). Thus, further examination of the ages and petrogenesis of these granitoids is required in order to understand the tectonic setting in which they were emplaced.

The Getengling pluton, located in northeastern Hunan Province (Figure 1) and representative of the Neoproterozoic S-type granites in the Jiangnan Orogen, is selected for such a study. Several previous studies have been carried out for this pluton, including geochronology and petrochemistry, but there are still uncertainties about its age and petrogenesis. HNBGMR (1988) reported a single-zircon evaporation U–Pb age of ca. 844 Ma and a biotite K–Ar age of ca. 1124 Ma for the Getengling pluton, whereas Wang *et al*. (2004) treated this and other Neoproterozoic granitoids in northeastern Hunan as the western extension of the Jiuling batholith in Jiangxi Province (Figure 1(a)), which has a zircon SHRIMP U–Pb age of 819 ± 9 Ma (Li *et al*. 2003a). As biotite K–Ar dating is susceptible to later thermal events, and single-zircon evaporation U–Pb dating is likely affected by inherited zircon, which is common in S-type granites, a more updated zircon U–Pb dating with *in-situ* techniques is desirable for the Getengling pluton. Based on whole-rock major and trace element geochemistry, Li *et al*. (2007a) suggested that the Getengling pluton was derived from partial melting of metapelites of the Lengjiaxi Group, whereas Wang *et al*. (2004) proposed a psammitic source in the Lengjiaxi Group for the magma. New geochemical data for the Getengling pluton, including whole-rock major and trace elements and Nd isotopes, and zircon Hf isotopes, were collected in this study for further petrogenetic analysis.

Although tectonic discrimination diagrams may not be reliable for individual magmatic rocks due to potential complication caused by mixed sources, as suggested by Li *et al*. (2003b, 2006) and Wang *et al*. (2010), they have been successfully applied to various tectonic settings worldwide based on statistics from large databases (Wood 1980; Pearce *et al*. 1996; Cawood *et al*. 2017). Therefore, in addition to the new geochemical studies of the Getengling granitoid, we have made a compilation of geochemical data of various magmatic rocks from the Jiangnan Orogen and plotted them on tectonic discrimination diagrams, thus providing a regional database to further constrain the petrogenesis and tectonic setting of the Getengling pluton. A sequential trend of tectonic evolution of the Jiangnan Orogen is revealed by this regional comparison, which, combined with previous studies on Neoproterozoic igneous rocks and sedimentary rocks in South China, Australia, and western Laurentia, provides new insights on the Neoproterozoic tectono-magmatic evolution of the South China Block.

2. Geological setting

The South China Block is composed of the Yangtze Block in the northwest and the Cathaysia Block in the southeast (present coordinates). The Jiangnan Orogen, an ENE–NE-trending Neoproterozoic continent–continent collisional belt, with a length of about 1500 km and a width of nearly 120 km, is located in the

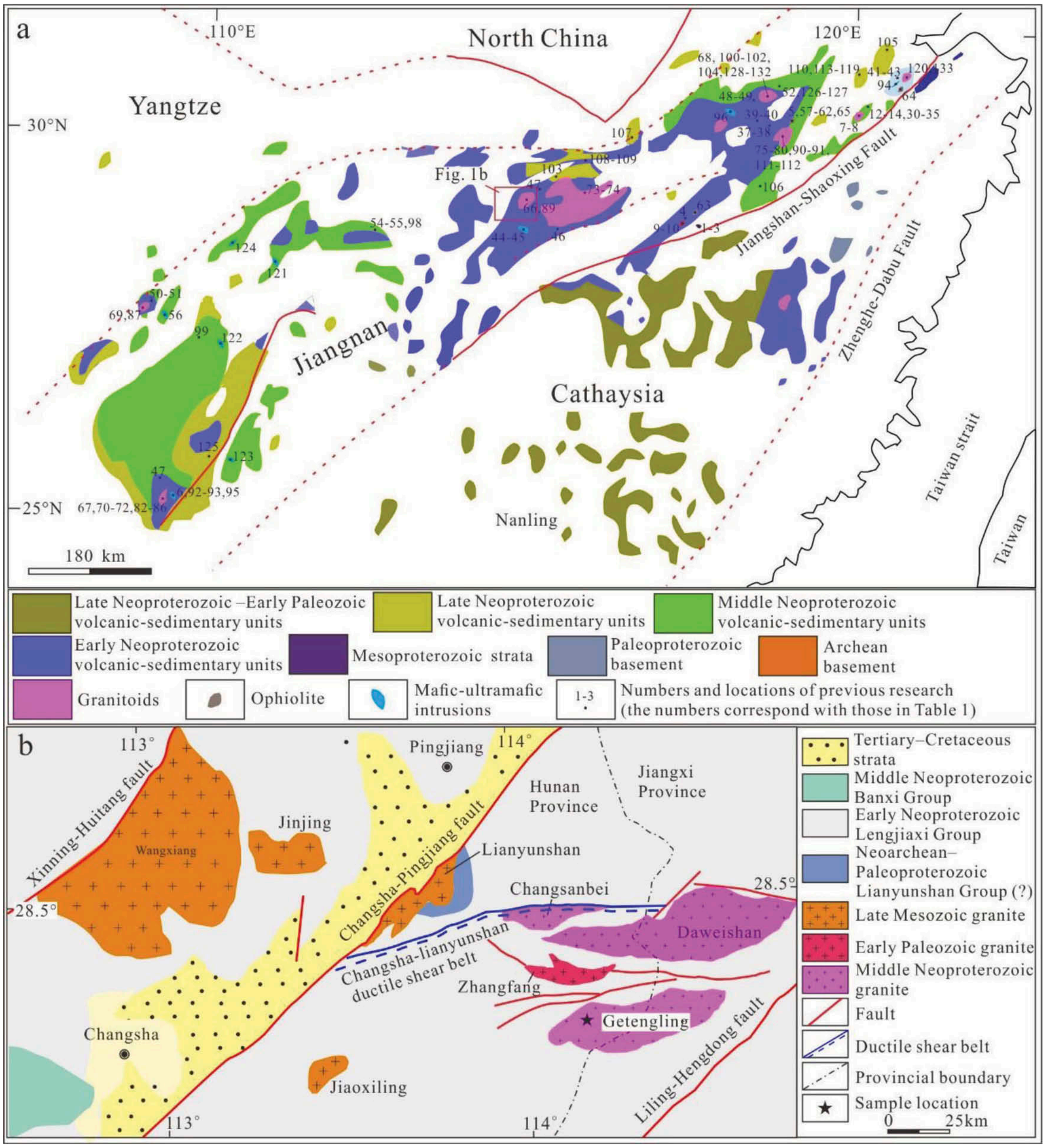

Figure 1. Simplified geological maps of (a) the Jiangnan Orogen (modified after Zhao and Cawood 2012) and (b) northeastern Hunan (Deng *et al.* 2017).

southeast margin of the Yangtze Block (Figure 1(a); Li *et al.* 2003a; Yao *et al.* 2014a).

The Jiangnan Orogen mainly consists of Neoproterozoic rocks, with minor Mesoproterozoic rocks. The Mesoproterozoic metasedimentary rocks are represented by the Tianli Schists in NE Jiangxi, which have a maximum depositional age of ca. 1530 Ma and went through two metamorphic events at ca. 1000 and ca. 960–940 Ma (Li *et al.* 2007b). The majority of the formations exposed in the Jiangnan Orogen are two sets of Neoproterozoic greenschist-facies metamorphosed volcanic-sedimentary rocks, which are given different names in different provinces (Figure 1(a); Zhou *et al.* 2002; Li *et al.* 2008c). The early Neoproterozoic rocks are named the Lengjiaxi Group in Hunan Province, Sibao Group in Guangxi Province, Fanjingshan Group in Guizhou Province, Shuangqiaoshan Group in Jiangxi Province, Shangxi Group in Anhui Province, and Shuangxiwu Group in Zhejiang Province. The unconformably overlying middle Neoproterozoic strata are called the Banxi, Danzhou, Xiajiang, Luokedong, and Likou groups in the different provinces (Wang *et al.* 2004; Xu *et al.* 2007; Wang *et al.* 2008c; Wang *et al.* 2012a; Li *et al.* 2007b, 2009; Zhao *et al.* 2011; Zhao and Cawood 2012). Recent geochronology studies show that the maximum depositional ages for the early Neoproterozoic strata are ca. 870–835 Ma, as constrained by the youngest detrital zircons of these strata (Wang *et al*. 2007; Wang *et al*. 2012a; Zhao *et al*. 2011), and the minimum depositional ages of these strata are ca. 815–800 Ma, as defined by the ages of volcanic rocks in the uncomfortably overlying middle Neoproterozoic strata (Wang *et al*. 2003; Gao *et al*. 2010b, 2011). The ages of the middle Neoproterozoic strata range from 815 Ma to younger than 730 Ma (Wang *et al*. 2003; Zhao *et al*. 2011).

Two major Neoproterozoic ophiolitic belts, i.e. the northeastern Jiangxi and Fuchuan ophiolitic mélange belts, have been recognized in the northeastern Jiangnan Orogen. Recent geochronological data suggest that the northeastern Jiangxi ophiolite was formed at ca. 1000 Ma (Chen *et al*. 1991; Shu *et al*. 1994; Li *et al*. 2008a; Gao *et al*. 2009; Deng et al. 2017), while the Fuchuan ophiolite was generated at ca. 848–819 Ma (Ding *et al*. 2008; Zhang *et al*. 2012a, 2013b). There are many pre-850 Ma mafic–felsic intrusions and volcanic rocks in the Jiangnan Orogen, some of which have adakitic signatures (Table 1). Most of them are interpreted as products of arc magmatism related to plate subduction in an active continent margin (Li 2003; Ye *et al*. 2007; Gao *et al*. 2009; Li *et al*. 2009; Chen *et al*. 2009a, 2016; Yao *et al*. 2014b). The 880 ± 19-Ma leucogranitic rocks in northeastern Jiangxi were interpreted as obduction related (Li *et al*. 2008a), and the ca. 906–904-Ma keratophyes in the Pingshui Group of Zhejiang Province were considered as the result of arc–continent collision by Chen *et al*. (2009b).

A number of ca. 850–820 Ma S-type granites intruding the Lengjiaxi Group and its equivalent strata occur in the Jiangnan Orogen (Figure 1(a)), including the Getengling, Daweishan, Changsanbei, and Zhangbangyuan plutons in Hunan (HNBGMR, 1988; Li *et al*. 2007a); the Jiuling pluton in Jiangxi (Li *et al*. 2003a); the Xucun, Shexian, and Xiuning plutons in Anhui (Wu *et al*. 2006a; Zheng *et al*. 2008, 2008b); the Tianpeng, Sanfang, Bendong, Yuanbaosha, Zhaigun, Dongma, and Tianpeng plutons in Guangxi (Li *et al*. 2003a; Wang *et al*. 2006); and the Motianling pluton in Guizhou (Ma *et al*. 2016). Latest zircon U–Pb dating demonstrates that these S-type granites were emplaced from ca. 835 to 800 Ma, with the majority clustered at ca. 835–820 Ma (Li *et al*. 2003a; Wang *et al*. 2006; Wu *et al*. 2006a; Zheng *et al*. 2008, 2008b; Zhao *et al*. 2011). Along with these, S-type granitic intrusions are some coeval mafic intrusions, which account for about 8% of the total intrusions in terms of exposure area (Li *et al*. 1999, 2008c; Wang *et al*. 2006; Zhou *et al*. 2007b; Zhou *et al*. 2009). There is also a number of post-820 Ma Neoproterozoic igneous rocks in the Jiangnan Orogen, including A- and S-type granites (Li *et al*. 2003b, 2008b; Wu *et al*. 2005; Zheng *et al*. 2008; Xue *et al*. 2010; Wang *et al*. 2012c; Yao *et al*. 2014a), mafic intrusions (Ge *et al*. 2001; Zhou *et al*. 2007a; Wang *et al*. 2012c), bimodal volcanic rocks, and other mafic–granitic volcanic rocks (Table 1; Wu *et al*. 2007; Zhou *et al*. 2007a; Li *et al*. 2008b; Wang *et al*. 2008c, Wang *et al*. 2012c; Zheng *et al*. 2008). The Getengling pluton is located in the middle part of the Jiangnan Orogen, half in Hunan Province and half in Jiangxi Province (Figure 1(b)), having a total exposure area of 114 km^2. It intruded into the Lengjiaxi Group (Figure 2(a)), which was locally migmatized (HNBGMR (Bureau of geology and mineral Resource of Hunan province) 1988).

3. Sample descriptions and analytical methods

3.1. Sample description

Eight fresh samples were collected from the Getengling pluton. The samples are grey medium–fine grained granites (Figure 2(a)). Major minerals include quartz (36–40 vol%), plagioclase (30–35 vol%), K-feldspar (10–15 vol%), biotite (~8 vol%), and muscovite (~5 vol%) (Figure 2(c–f)). Petrographic classification diagram shows that the samples are granodiorites (Figure 3(a)). Quartz commonly shows wavy extinction and has grain sizes ranging from 0.2 to 1.5 mm (Figure 2(c)). K-feldspar is characterized with contact twinning and plagioclase with polysynthetic twinning, and they have some extents of sericitization. K-feldspar and plagioclase have grain sizes of 0.4–0.8 and 0.3–1 mm, respectively (Figure 2(d,e)). Muscovite grains (with some being secondary) have sizes of 0.1–1.3 mm (Figure 2(c,d)), and biotite grains have sizes of 0.2–1 mm and eminent cleavages (Figure 2(c–f)).

3.2. Analytical methods

3.2.1. Whole-rock major and trace elementary geochemistry

Whole-rock major and trace element analyses were carried out at the State Key Laboratory of Isotope Geochemistry, Guangzhou Institute of Geochemistry, Chinese Academy of Sciences (GIGCAS). Fresh rock samples were crushed to centimetre-size grains, washed with HNO_3, dried, and then milled to below 200-mesh powder. Sample powder was melted with $Li_2B_4O_7$ (1:8) to make homogeneous glass discs at 1250°C using a V8C automatic fusion machine. The major elements were measured with the X-ray fluorescence spectrometry technique (Rigaku 100e). Analytical errors for the major elements were better than 1%. Aliquots of the

Table 1. List of existing and new ages for the Proterozoic strata and igneous rocks in the Jiangnan Orogen.

Number	Rock	Location	Age (Ma)	Method	Reference
1	Tianli Schists	Northeast Jiangxi	1530	Zircon SHRIMP U–Pb (the youngest detrital zircons)	Li *et al.* (2007b)
2	Tianli Schists	Northeast Jiangxi	1042–1015	Ar–Ar on S_1 muscovite	Li *et al.* (2007b)
3	Tianli Schists	Northeast Jiangxi	966 ± 4	Ar–Ar on S_2 muscovite	Li *et al.* (2007b)
4	Blueschist	Northeast Jiangxi	866 ± 14	Glaucophaen K–Ar	Shu *et al.* (1994)
5	Gabbro	Fuchuan, northeast Jiangxi	875 ± 8	Zircon LA-ICP-MS U–Pb	Zhang *et al.* (2013a)
6	Gabbro	Yuanbaoshan, Northeast Jiangxi	854.7 ± 5.3	Zircon LA-ICP-MS U–Pb	Yao *et al.* (2014b)
7	Taohong I-type granite	Northeast Zhejiang	913 ± 15	Zircon SHRIMP U–Pb	Ye *et al.* (2007)
8	Xiqiu I-type granite	Northeast Zhejiang	905 ± 14	Zircon SHRIMP U–Pb	Ye *et al.* (2007)
9	Xiwan adakitic granite	Northeast Jiangxi	970 ± 21	Zircon SHRIMP U–Pb	Gao *et al.* (2009)
10	Xiwan adakitic granite	Northeast Jiangxi	968 ± 23	Zircon SHRIMP U–Pb	Li (2003)
11	High-Mg diorite	Pingshui area, northeast Zhejiang	932 ± 7	Zircon LA-ICP-MS U–Pb	Chen *et al.* (2009a)
12	Nb-enriched basaltic porphyry	Pingshui area, northeast Zhejiang	916 ± 6	Zircon LA-ICP-MS U–Pb	Chen *et al.* (2009a)
13	Plagiogranite	Pingshui area, northeast Zhejiang	902 ± 5	Zircon LA-ICP-MS U–Pb	Chen *et al.* (2009a)
14	'Obduction-type' granite	Xiwan, northeast Jiangxi	880 ± 19	Zircon SHRIMP U–Pb	Li *et al.* (2008a)
15	Sibao Group	Guangxi	868.2 ± 9.7	Zircon LA-ICP-MS U–Pb (the youngest detrital zircons)	Wang *et al.* (2007)
16	Sibao Group	Guangxi	835.3 ± 3.6	Zircon LA-ICP-MS U–Pb (the youngest detrital zircons)	Wang *et al.* (2012a)
17	Sibao Group	Guangxi	834.9 ± 3.8	Zircon LA-ICP-MS U–Pb (the youngest detrital zircons)	Ma *et al.* (2016)
18	Lengjiaxi Group	Hunan	862 ± 11	Zircon LA-ICP-MS U–Pb (the youngest detrital zircons)	Wang *et al.* (2007)
19	Fanjinshan Group	Guizhou	872 ± 3	Zircon LA-ICP-MS U–Pb (the youngest detrital zircons)	Zhou *et al.* (2009)
20	Lengjiaxi Group	Hunan	ca. 878–879	Zircon LA-ICP-MS U–Pb (the youngest detrital zircons)	Zhao *et al.* (2011)
21	Sibao Group	Guangxi	ca. 865–872	Zircon LA-ICP-MS U–Pb (the youngest detrital zircons)	Zhao *et al.* (2011)
22	Shuangqiaoshan Group	Jiangxi	ca. 849–871	Zircon LA-ICP-MS U–Pb (the youngest detrital zircons)	Zhao *et al.* (2011)
23	Shuangqiaoshan Group	Jiangxi	ca. 831–815	Zircon LA-ICP-MS U–Pb (the youngest detrital zircons)	Wang *et al.* (2013b)
24	Xikou Group	Southern Anhui	ca. 833–817	Zircon LA-ICP-MS U–Pb (the youngest detrital zircons)	Wang *et al.* (2013b)
25	Xikou Group	Southern Anhui	842 ± 10	Zircon LA-ICP-MS U–Pb (the youngest detrital zircons)	Yin *et al.* (2013)
26	Xingzi Group	Northwest Jiangxi	ca. 820–810	Zircon LA-ICP-MS U–Pb	Wang *et al.* (2016)
27	Kangwanggu Group	Northwest Jiangxi	ca. 830	Zircon LA-ICP-MS U–Pb	Wang *et al.* (2016)
28	Qigong Group	Yiyang area, Hunan	ca. 830	Zircon LA-ICP-MS U–Pb	Yao *et al.* (2013)
29	Hongchi greywacke	Yiyang area, Hunan	ca. 860	Zircon LA-ICP-MS U–Pb	Yao *et al.* (2013)
30	Spilite in Pingshui Group	Northwest Zhejiang	952 ± 5	Zircon LA-ICP-MS U–Pb	Chen *et al.* (2016)
31	Keratophye in Pingshui Group[a]	Northwest Zhejiang	954 ± 8	Zircon LA-ICP-MS U–Pb	Chen *et al.* (2016)
32	Keratophye in Pingshui Group[b]	Zhejiang	904 ± 8	Zircon LA-ICP-MS U–Pb	Chen *et al.* (2009b)
33	Keratophye in Pingshui Group[b]	Zhejiang	906 ± 10	Zircon LA-ICP-MS U–Pb	Chen *et al.* (2009b)
34	Beiwu andesitic rock	Fuyang, eastern Zhejiang	926 ± 15	Zircon SHRIMP U–Pb	Li *et al.* (2009)
35	Zhangcun rhyolitic rock	Fuyang, eastern Zhejiang	891 ± 12	Zircon SHRIMP U–Pb	Li *et al.* (2009)
36	Olistostrome of andesite	Northeast Jiangxi	871 ± 7	Zircon LA-ICP-MS U–Pb	Yao *et al.* (2015)
37	Olistostrome of andesite	Northeast Jiangxi	868 ± 7	Zircon LA-ICP-MS U–Pb	Yao *et al.* (2015)
38	Olistostrome of andesite	Northeast Jiangxi	864 ± 14	Zircon LA-ICP-MS U–Pb	Yao *et al.* (2015)
39	Quartz-keratophyre in the bottom of Shuangqiaoshan Group	Jiangxi	878 ± 5	Zircon SHRIMP U–Pb	Wang *et al.* (2008b)
40	Tuff in the bottom of Shuangqiaoshan Group	Jiangxi	879 ± 6	Zircon SHRIMP U–Pb	Wang *et al.et al.* (2008b)
41	Dolerite	Shuige, Hangzhou, eastern Zhejiang	863 ± 6	Zircon LA-ICP-MS U–Pb	Yao *et al.* (2014a)
42	Huangshan bimodal volcanic rocks	Zhejiang	860 ± 9	Zircon SIMS U–Pb	Lyu *et al.* (2017)
43	Meiling bimodal volcanic rocks	Zhejiang	840 ± 5	Zircon SIMS U–Pb	Lyu *et al.* (2017)

(*Continued*)

Table 1. (Continued).

Number	Rock	Location	Age (Ma)	Method	Reference
44	Shuikou basalt	Northeast Hunan	860 ± 20	Zircon SHRIMP U–Pb	Zhang *et al.* (2013b)
45	Nanqiao basalt	Northeast Hunan	838 ± 12	Zircon SIMS U–Pb	Zhang *et al.* (2013b)
46	Fangxi dolerite	Northwest Jiangxi	847 ± 18	Zircon LA-ICP-MS U–Pb	Zhang *et al.* (2013b)
47	Bentonite in Sibao Group	Guangxi	841.7 ± 5.9	Zircon SHRIMP U–Pb	Gao *et al.* (2010a)
48	Dacite	Shiershan, Anhui	825 ± 11	Zircon LA-ICP-MS U–Pb	Zheng *et al.* (2008)
49	Dacite	Shiershan, Anhui	820 ± 16	Zircon LA-ICP-MS U–Pb	Zheng *et al.* (2008)
50	Volcanic rock in Fanjinshan Group	Guizhou	831 ± 4	Zircon LA-ICP-MS U–Pb	Zhao *et al.* (2011)
51	Volcanic rock in Fanjinshan Group	Guizhou	827 ± 15	Zircon LA-ICP-MS U–Pb	Zhao *et al.* (2011)
52	Dacite of Jingtan Formation in Shangxi Group	Anhui	820 ± 16	Zircon SHRIMP U–Pb	Wu *et al.* (2007)
53	Bentonite in Lengjiaxi Group	Hunan	822 ± 10	Zircon SHRIMP U–Pb	Gao *et al.* (2011)
54	Cangshuipu andesite	Hunan	822 ± 28	Zircon SHRIMP U–Pb	Zhang *et al.* (2012b)
55	Cangshuipu andesite	Hunan	824 ± 7	Zircon SIMS U–Pb	Zhang *et al.* (2012b)
56	Mafic rock	Guizhou	822 ± 15	Zircon LA-ICP-MS U–Pb	Zhou *et al.* (2009)
57	Gabbro	Fuchuan ophiolite, Anhui	819 ± 3	Zircon LA-ICP-MS U–Pb	Zhang *et al.* (2013a)
58	Gabbro	Fuchuan ophiolite, Anhui	827 ± 3	Zircon LA-ICP-MS U–Pb	Zhang *et al.* (2013a)
59	Gabbro	Fuchuan ophiolite, Anhui	822 ± 3	Zircon LA-ICP-MS U–Pb	Zhang *et al.* (2013a)
60	Gabbro	Fuchuan ophiolite, Anhui	824 ± 3	Zircon SHRIMP U–Pb	Zhang *et al.* (2012a)
61	Gabbro	Fuchuan ophiolite, Anhui	827 ± 9	Zircon SHRIMP U–Pb	Ding *et al.* (2008)
62	Gabbro	Fuchuan ophiolite, Anhui	848 ± 12	Zircon SHRIMP U–Pb	Ding *et al.* (2008)
63	Anorthosite	Northeast Jiangxi ophiolite	968 ± 23	Zircon SHRIMP U–Pb	Li *et al.* (1994)
64	Zhuji gabbro	Western Zhejiang ophiolite	858 ± 11	Zircon SHRIMP U–Pb	Shu *et al.* (2006)
65	Gabbro	Fuchuan ophiolite, Anhui	1024 ± 30	Whole-rock Sm–Nd isochron	Zhou *et al.* (1990)
66	**Getengling S-type granite**	**Northeast Hunan**	**845 ± 4**	**Zircon LA-ICP-MS U–Pb**	**This paper**
67	Yuanbaoshan S-type granite	Guangxi	828 ± 5	Zircon LA-ICP-MS U–Pb	Yao *et al.* (2014b)
68	S-type granite	Shier mountain, Anhui	822 ± 12	Zircon LA-ICP-MS U–Pb	Zheng *et al.* (2008)
69	S-type granite in Fanjinshan Group[a]	Guizhou	838 ± 2	Zircon LA-ICP-MS U–Pb	Wang *et al.* (2011a)
70	Zhaigun S-type granite	Guangxi	836 ± 3	Zircon LA-ICP-MS U–Pb	Wang *et al.* (2006)
71	Dongma S-type granite	Northern Guangxi	824 ± 13	Zircon LA-ICP-MS U–Pb	Wang *et al.* (2006)
72	Tianpeng S-type granite	Northern Guangxi	794.2 ± 8.1	Zircon LA-ICP-MS U–Pb	Wang *et al.* (2006)
73	Jiuling S-type granite	Jiangxi	820 ± 10	Zircon SHRIMP U–Pb	Zhong *et al.* (2005)
74	Jiuling S-type granite	Jiangxi	819 ± 9	Zircon SHRIMP U–Pb	Li *et al.* (2003a)
75	Xucun S-type granite	Southern Anhui	823 ± 8	Zircon SHRIMP U–Pb	Li *et al.* (2003a)
76	Xiuning S-type granite	Southern Anhui	824–825	Zircon LA-ICP-MS U–Pb	Wu *et al.* (2006a)
77	Shexian S-type granite	Southern Anhui	823–824	Zircon LA-ICP-MS U–Pb	Wu *et al.* (2006a)
78	Shexian S-type granite	Southern Anhui	838 ± 11	Zircon LA-ICP-MS U–Pb	Xue *et al.* (2010)
79	Xucun S-type granite	Southern Anhui	850 ± 10	Zircon LA-ICP-MS U–Pb	Xue *et al.* (2010)
80	Xucun S-type granite	Southern Anhui	823–827	Zircon LA-ICP-MS U–Pb	Wu *et al.* (2006)
81	Eshan S-type granite	Yunan	819 ± 8	Zircon SHRIMP U–Pb	Li *et al.* (2003a)
82	S-type granite in Sibao Group	Guangxi	826.8 ± 5.9	Zircon SHRIMP U–Pb	Gao *et al.* (2010a)
83	Bendong S-type granite	Guangxi	819 ± 9	Zircon SHRIMP U–Pb	Li (1999)

(*Continued*)

Table 1. (Continued).

Number	Rock	Location	Age (Ma)	Method	Reference
84	Bendong S-type granite	Guangxi	823 ± 3.8	Zircon LA-ICP-MS U–Pb	Wang *et al.* (2006)
85	Sanfang S-type granite	Guangxi	826 ± 10	Zircon SHRIMP U–Pb	Li (1999)
86	Sanfang S-type granite	Guangxi	804.3 ± 5.2	Zircon LA-ICP-MS U–Pb	Wang *et al.* (2006)
87	S-type granite in Fanjinshan Group[b]	Guizhou	827.5 ± 7.4	Zircon SIMS U–Pb	Zhao *et al.* (2011)
88	Motianling S-type granite	Guizhou	825.6 ± 3.0	Zircon LA-ICP-MS U–Pb	Ma *et al.* (2016)
89	Zhangbangyuan granite	Northeast Hunan	816 ± 4.6	Zircon SHRIMP U–Pb	Ma *et al.* (2009)
90	Shexian S-type granite	Southern Anhui	838 ± 11	Zircon LA-ICP-MS U–Pb	Xue *et al.* (2010)
91	Xiuning S-type granite	Southern Anhui	832 ± 8	Zircon LA-ICP-MS U–Pb	Xue *et al.* (2010)
92	Mafic–ultramafic dike and sill	Sanfang, Guangxi	828 ± 7	Zircon SHRIMP U–Pb	Li *et al.* (1999)
93	Mafic rock	Yuanbaoshan, Guangxi	841 ± 22	Zircon SHRIMP U–Pb	Zhou *et al.* (2007b)
94	Shenwu dolerite dike	Northern Zhejiang	849 ± 7	Zircon SHRIMP U–Pb	Li *et al.* (2008b)
95	Hejiawan layered diabase	Guangxi	811.5 ± 4.8	Zircon LA-ICP-MS U–Pb	Wang *et al.* (2006)
96	Gabbro of Shuangqiaoshan Group	Jiangxi	801 ± 4	Zircon SHRIMP U–Pb	Wang *et al.* (2008b)
97	Volcanic and clastic rock overlying Tianli Schists	Northeast Jiangxi	818 ± 12	Zircon SHRIMP U–Pb	Wang *et al.* (2003)
98	Cangshuipu dacitic volcanic conglomerate	Base of Banxi Group in northeast Hunan	814 ± 12	Zircon SHRIMP U–Pb	Wang *et al.* (2003)
99	Bentonite in Xiajiang Group	Guizhou	814 ± 6.3	Zircon SHRIMP U–Pb	Gao *et al.* (2010b)
100	Lingshan granite	Anhui	823 ± 18	Zircon LA-ICP-MS U–Pb	Xue *et al.* (2010)
101	Lianhuashan granite	Anhui	814 ± 26	Zircon LA-ICP-MS U–Pb	Xue *et al.* (2010)
102	Youershan	Anhui	783 ± 8	Zircon LA-ICP-MS U–Pb	Xue *et al.* (2010)
103	Bentonite in Banxi Group	Northeast Hunan	802.6 ± 7.6	Zircon SHRIMP U–Pb	Gao *et al.* (2011)
104	Granite	Shier mountain, Anhui	779 ± 11	Zircon SHRIMP U–Pb	Li *et al.* (2003b)
105	Hongchicun intermediate to felsic volcanic rock	Zhejiang	797 ± 11	Zircon SHRIMP U–Pb	Li *et al.* (2003b)
106	Bimodal volcanic rocks	Northeast Jiangxi	803 ± 9	SHRIMP	Wang *et al.* (2015)
107	Lushanlong rhyolite	Northeast Jiangxi	ca. 827–829	LA-ICP-MS	Wang *et al.* (2016)
108	Xingzi amphibolites	Lushan, Jiangxi	811 ± 12	SHRIMP	Li *et al.* (2013)
109	Shaojiwa rhyolite	Lushan, Jiangxi	828 ± 6	SHRIMP	Li *et al.* (2013)
110	Shangshu bimodal volcanic rock	Northern Zhejiang	792 ± 5	Zircon SHRIMP U–Pb	Li *et al.* (2008b)
111	Granite porphyry of Xucun composite dikes	Southern Anhui	805 ± 4	Zircon LA-ICP-MS U–Pb	Wang *et al.* (2012c)
112	Diabase of Xucun composite dikes	Southern Anhui	804 ± 7	Zircon LA-ICP-MS U–Pb	Wang *et al.* (2012c)
113	Shangshu basalt	Northeast Jiangxi	802 ± 8	Zircon LA-ICP-MS U–Pb	Wang *et al.* (2012c)
114	Shangshu dacite	Southern Anhui	794 ± 7	Zircon LA-ICP-MS U–Pb	Wang *et al.* (2012c)
115	Shangshu rhyolitic porphyry	Southern Anhui	797 ± 6	Zircon LA-ICP-MS U–Pb	Wang *et al.* (2012c)
116	Shangshu rhyolite	Between southern Anhui and northeast Jiangxi	797 ± 5	Zircon LA-ICP-MS U–Pb	Wang *et al.* (2012c)
117	Rhyolite in Puling Formation	Anhui	765 ± 7	Zircon LA-ICP-MS U–Pb	Wang *et al.* (2012c)
118	Tuff in Puling Formation	Anhui	751 ± 8	Zircon LA-ICP-MS U–Pb	Wang *et al.* (2012c)
119	Tuff in Puling Formation	Anhui	763 ± 12	Zircon LA-ICP-MS U–Pb	Wang *et al.* (2012c)
120	A-type granite	Daolinshang, Jiangxi	790 ± 5	Zircon LA-ICP-MS U–Pb	Yao *et al.* (2014a)
121	Qianyang diabase	Western Hunan	747 ± 18	Zircon SHRIMP U–Pb	Wang *et al.* (2008b)
122	Tongdao altered ultramafic rock	Western Hunan	756 ± 12	Zircon SHRIMP U–Pb	Wang *et al.* (2008b)
123	Longsheng gabbro–diabase	Northern Guanagxi	761 ± 8	Zircon TIMS Pb–Pb concordant age	Ge *et al.* (2001)
124	Guzhang diabase	Western Hunan	768 ± 28	Zircon SHRIMP U–Pb	Zhou *et al.* (2007a)
125	Sanmenjie Rhyo-dacite	Northern Guanagxi	765 ± 14	Zircon SHRIMP U–Pb	Zhou *et al.et al.* (2007a)
126	Dacite of Jingtan Formation	Southern Anhui	773 ± 7	Zircon LA-ICP-MS U–Pb	Wu *et al.* (2007)

(Continued)

Table 1. (Continued).

Number	Rock	Location	Age (Ma)	Method	Reference
127	Tuff of Jingtan Formation	Western Zhejiang	779 ± 7	Zircon LA-ICP-MS U–Pb	Zheng *et al.* (2008)
128	Granite in Shiershan	Southern Anhui	771 ± 17	Zircon LA-ICP-MS U–Pb	Zheng *et al.* (2008)
129	Granite in Shiershan	Southern Anhui	777 ± 7	Zircon LA-ICP-MS U–Pb	Zheng *et al.* (2008)
130	Granite in Shiershan	Southern Anhui	775 ± 5	Zircon LA-ICP-MS U–Pb	Zheng *et al.* (2008)
131	Granite in Shiershan	Southern Anhui	777 ± 9	Zircon LA-ICP-MS U–Pb	Wu *et al.* (2005)
132	Granite in Shiershan	Southern Anhui	779 ± 11	Zircon SHRIMP U–Pb	Li *et al.* (2003b)
133	Daolinshan A-type granite	Northern Zhejiang	794 ± 9	Zircon SHRIMP U–Pb	Li *et al.* (2008b)
134	Xiajiang Group	Congjiang, southeast Guizhou	794.6 ± 4.2	LA-ICP-MS	Ma *et al.* (2016)
135	Xiuning Formation	Southern Anhui	763 ± 10	LA-ICP-MS	Wang *et al.* (2013a)
136	Xiajiang Group	Northeast Guizhou	741 ± 6	LA-ICP-MS	Wang *et al.* (2010)
137	Danzhou Group	Northern Guangxi	730–770	LA-ICP-MS	Wang *et al.* (2012)
138	Nanhua Sequence	Southern Anhui	751 ± 8	LA-ICP-MS	Wang *et al.* (2013b)
139	Nanhua Sequence	Southern Anhui	753 ± 8	LA-ICP-MS	Wang *et al.* (2013b)
140	Xiajiang Group	Guizhou	770–800	SIMS	Wang *et al.* (2012b)
141	Chang'an Formation, Jiangkou Group	Guizhou	750–799	SIMS	Wang *et al.* (2012b)
142	Banxi Group	Hunan	782.3 ± 4.3	SIMS	Wang *et al.* (2012b)
143	Danzhou Group	Guangxi	731.3 ± 4.4	SIMS	Wang *et al.* (2012b)
144	Dengshan greywacke (covering sequence)	Yiyang, Hunan	ca. 745	LA-ICP-MS	Yao *et al.* (2013)

The data from this study are highlighted in bold.
[a,b] To differenciate the different rocks with the same name.

same sample powders were used for trace element analysis with ICP-MS, following the procedures of Liu *et al.* (1996). Analytical uncertainty of the elements was better than 5%, except for few samples with low contents of trace elements, for which the uncertainty was about 10%. The obtained values of the trace and REE elements in the standards are all consistent with their recommended values reported by Liu *et al.* (1996).

3.2.2. Zircon U–Pb dating

Zircon U–Pb dating was conducted using the laser ablation inductively coupled plasma mass spectrometry (LA-ICP-MS) system at the State Key Laboratory of Isotope Geochemistry, GIGCAS. The U–Pb and trace elements of the zircons were analysed with an Agilent 7500a ICP-MS and a Resonetics Resolution M-50 laser-ablation system. The conditions were 80 mJ laser energy, a repetition rate of 8 Hz with a spot size of 31 μm in diameter, and 50 s ablation time (Li *et al.* 2012). To optimize data quality, a two-volume laser-ablation cell and a squid smoothing device were used (Tu *et al.* 2011; Li *et al.* 2012). The external calibration standards are PLESOVICE and TEMORA. PLESOVICE was analysed twice for every 10 analyses and TEMORA was analysed twice for every 5 analyses (Tu *et al.* 2011; Li *et al.* 2012). The internal standard used to calculate the content of trace elements is ^{29}Si. The analytical results were processed with ICPMSDataCal 7.4 (Liu *et al.* 2010a, 2010b), and U–Pb ages were calculated with Isoplot 3.23 (Ludwig 2004). The single spot data error is expressed in 1σ, and that for weighted average, $^{206}Pb/^{238}U$ age is in 2σ. The obtained mean weighted $^{206}Pb/^{238}U$ age (416.3 ± 3.2 Ma, 2σ, MSWD = 0.5) from all the TEMORA zircons is consistent with the recommended age of 416.75 ± 0.24 (Black *et al.* 2003).

3.2.3. Nd isotope

Whole-rock Nd isotopic ratios of the Getengling pluton samples were measured using a multi-collector inductively coupled plasma mass spectrometry at the State Key Laboratory of Isotope Geochemistry, GIGCAS, following the procedures of Wei *et al.* (2002) and Liang *et al.* (2003). Measured $^{143}Nd/^{144}Nd$ values were normalized to $^{146}Nd/^{144}Nd = 0.7129$ for mass fractionation. The measured value of the Nd standards (JNdi-1) is 0.512092 ± 7, which is consistent with the recommended values of 0.512080–0.512120.

3.2.4. Zircon Hf isotope

In-situ zircon Hf isotopic analysis of the Getengling pluton samples was carried out using a Geolas-193 laser-ablation microprobe at the State Key Laboratory of Isotope Geochemistry, GIGCAS. The laser ablation for Hf isotope

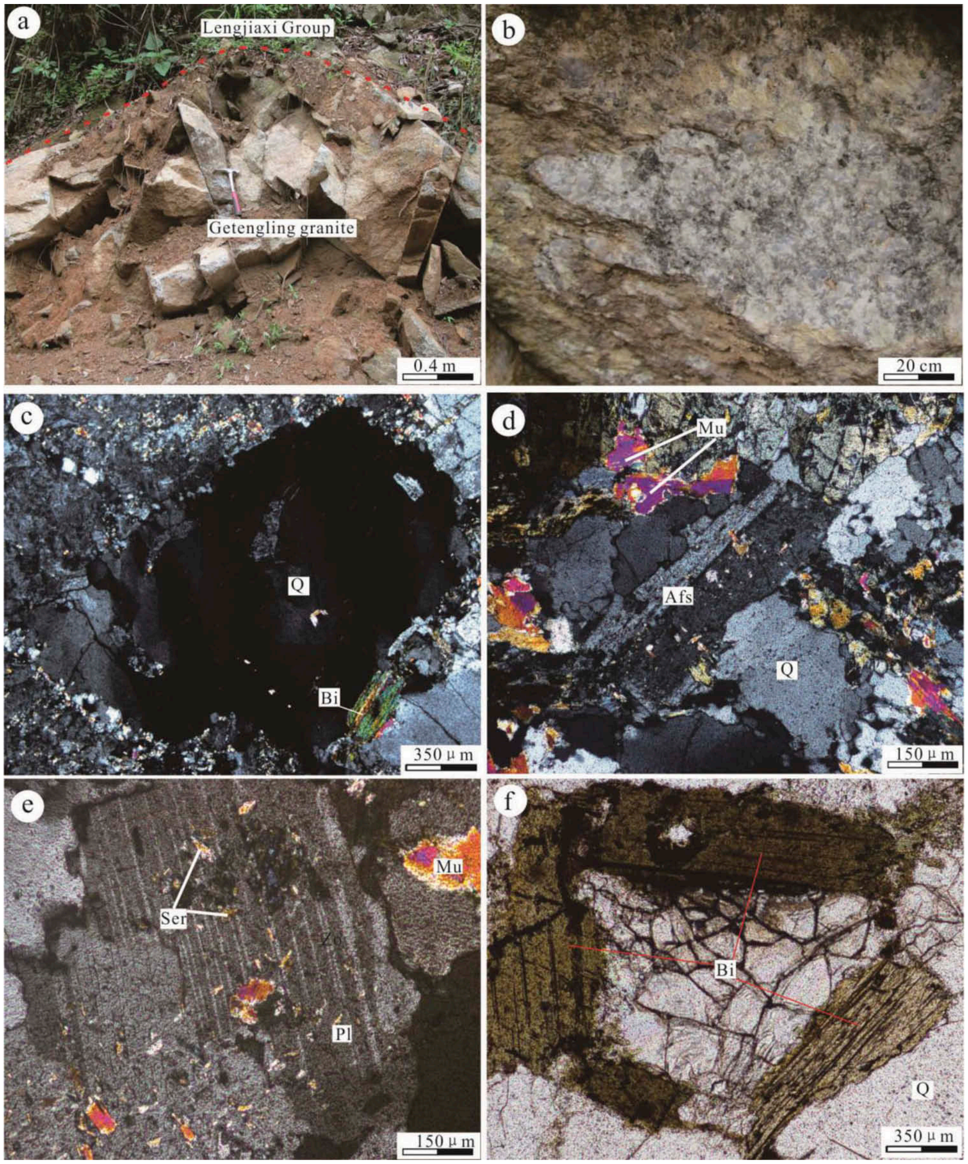

Figure 2. Thin section photographs of the Getengling pluton. (a) Quartz is well preserved and shows clear wavy extinction, and there are also biotite and feldspar (cross-polarized light). (b) Alkali feldspar with simple contact twinning (cross-polarized light), and there are abundant muscovite (cross-polarized light). (c) Plagioclase has polysynthetic twinning. (d) Large and abundant biotite grains (plain-polarized light). Q: Quartz; Pl: plagioclase; Afs: alkali feldspar; Bi: biotite; Mu: muscovite; Ser: sericite.

analysis was carried out on the same or approximate spot as that for U–Pb analysis, which was shown in Figure 4. A spot size of 40 μm and a 10-Hz repetition rate were used for analyses. The analytical procedures have been described previously in detail by Wu *et al*. (2006b). External calibration was made by measuring zircon standard Penglai to evaluate the reliability of the analytical data, which yielded a weighted mean ^{176}Hf/^{177}Hf ratio of 0.282891 ± 28 (2σ). This value is in good agreement with the recommended value of 0.2828906 ± 10 (2σ, Li *et al*. 2010a). The mean βYb value was applied for the isobaric interference correction of ^{176}Yb on ^{176}Hf in the same spot.

4. Results

4.1. Zircon U–Pb dating

U–Pb isotopic analyses were carried out on 39 zircon grains from sample SZT07 (Supplementary Table 1). Most of the zircon grains with lengths of up to 200 μm and length-to-width ratios between 1.5:1 and 2:1 are euhedral. These zircon grains show fine oscillatory zoning and contain inherited cores (Figure 4). The rims have variable abundances of Th ranging from 58 to 1786 ppm and U from 203 to 650 ppm, with Th/U ratios from 0.18 to 4.26. The inherited cores have

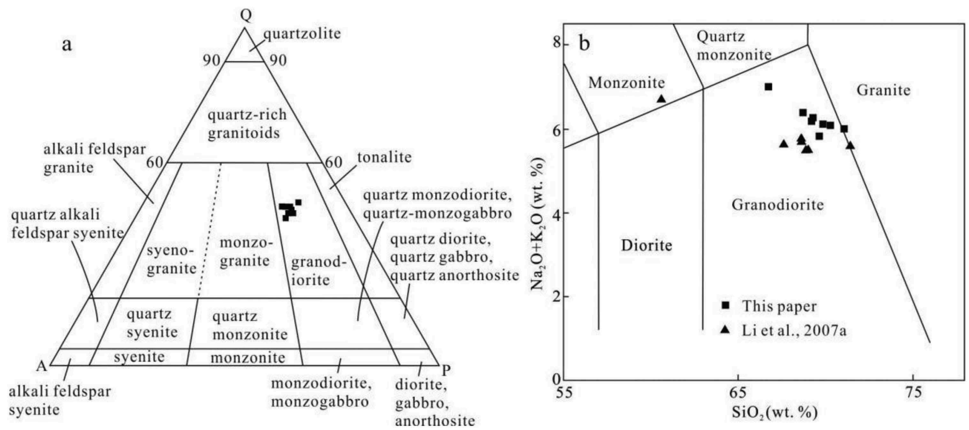

Figure 3. (a) QAP diagram and (b) TAS classification (modified after Middlemost 1994) for the Getengling pluton.

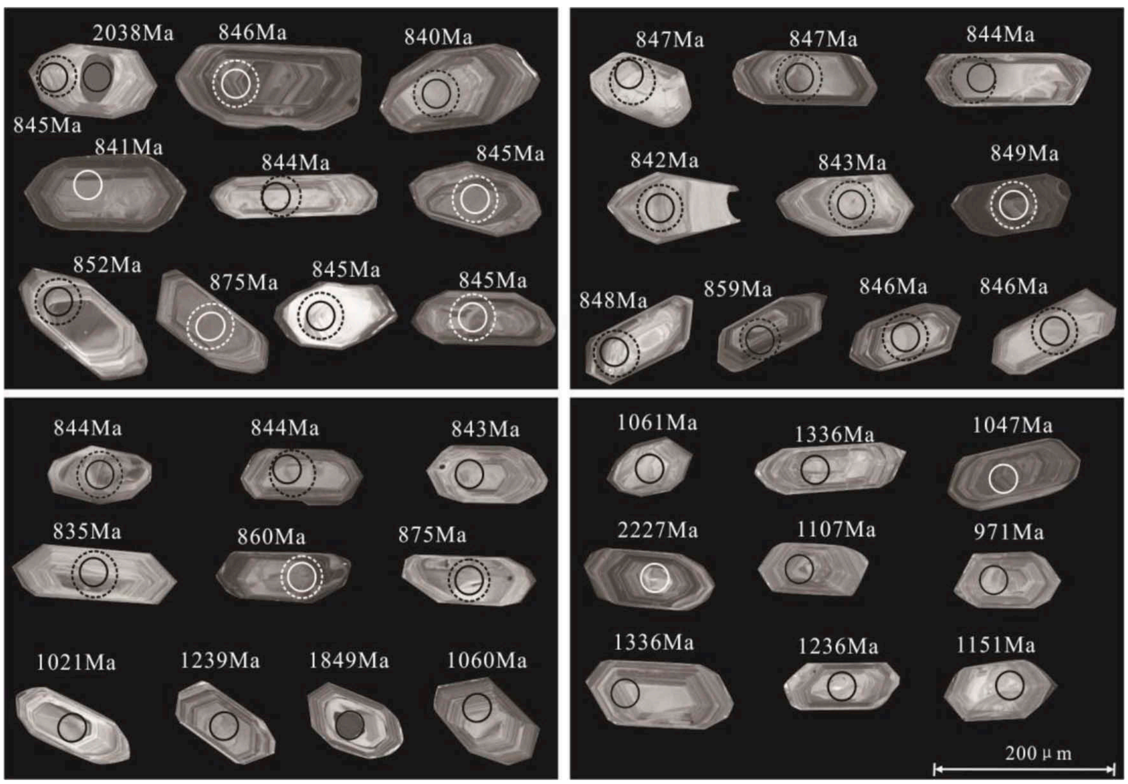

Figure 4. Cathodoluminescence (CL) images of zircons from the Getengling pluton with $^{206}Pb/^{238}U$ ages are also shown. Smaller solid spots mark the locations of LA-ICP-MS U–Pb dating and large dotted spots mark the locations of MC-LA-ICP-MS Hf isotope analyses.

similar abundances of Th (65–479 ppm) and U (197–627 ppm), with Th/U ratios ranging from 0.15 to 0.96. Most of the inherited cores have ages from ca. 1350 to 1000 Ma, except for two old ages of 2227 and 2038 Ma. For the spots in the rim, three were excluded from age calculation because they have <90% concordance (spots SZT07-18, SZT07-39, and SZT07-40). Three additional spots, whose ages are either significantly older (SZT07-1 and SZT07-27), possibly affected by older cores, or significantly younger (SZT07-36) than other spots in the rim, are excluded as well. For the remaining 20 analyses, $^{206}Pb/^{238}U$ ratios agree internally within analytical precision and yield a mean $^{206}Pb/^{238}U$ age of 845 ± 4 Ma (Figure 5(a)), indicating that the Getengling granodiorite is of Neoproterozoic age (Figure 5(b)).

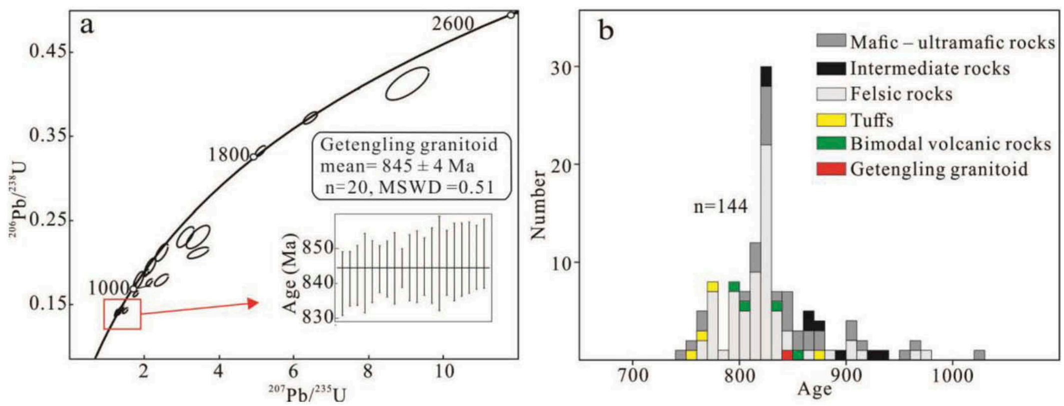

Figure 5. (a) Zircon LA-ICP-MS U–Pb age of the Getengling pluton; (b) histogram for the ages of Proterozoic igneous rocks in the Jiangnan Orogen. The ages' values are from Table 1.

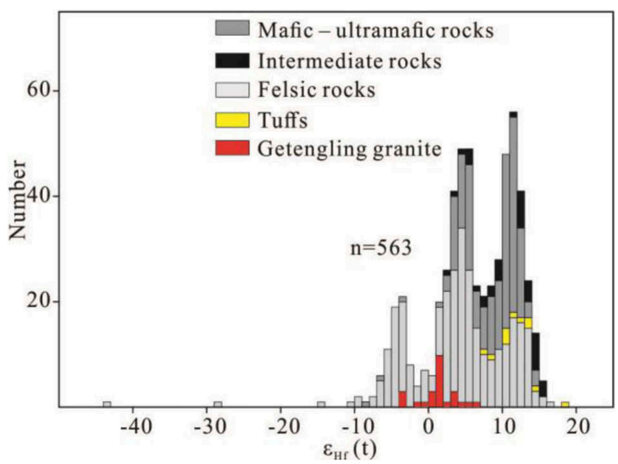

Figure 6. Histogram for zircon $\varepsilon_{Hf}(t)$ values of the Proterozoic igneous rocks in the Jiangnan Orogen. The $\varepsilon_{Hf}(t)$ values of the Getengling granitoid are from this paper, while others are from Wu *et al.* (2006a), Zheng *et al.* (2008), Wang *et al.* (2008b), Wang *et al.* (2012c), Li *et al.* (2009), Zhou *et al.* (2009), Chen *et al.* (2009a), Zhang *et al.* (2012a, 2012b, 2013a), and Yao *et al.* (2014a, 2014b, 2015).

4.2. *Zircon Hf isotope*

Lu–Hf isotopic analyses were performed on the 24 zircon grains from Sample SZT-07 (Supplementary Table 2). Initial $^{176}Hf/^{177}Hf$ and $\varepsilon_{Hf}(t)$ values were calculated at t = 845 Ma. Most spots show positive $\varepsilon_{Hf}(t)$ values of −4.9–6.3, with a weighted mean of 0.7 ± 1.1, lying in the range of other igneous rocks in the Jiangnan Orogen (Figure 6). The single-stage Hf model age (T_{DM1}) is 1.61–1.17 Ga, with a weighted mean of 1.36 ± 0.04 Ga.

4.3. *Major and trace element geochemistry*

Major and trace element geochemical data for the Getengling pluton are listed in Supplementary Table 3, and the data are generally consistent with those of Li *et al.* (2007a). The samples have loss on ignition (LOI) values of 1.29–2.15%, indicating minor effects of secondary hydrothermal alteration and/or metamorphism. Zr in igneous rocks is considered an immobile element during low-to-medium-grade metamorphism and alteration (Li *et al.* 2009). Al_2O_3, CaO, KO_2, Sr, Rb, Y, and Nb contents do not change significantly, and Na_2O and Ba contents decrease slightly with those of Zr (Supplementary Figure 1), suggesting minimal metamorphic and alteration effects on these elements, thus suitable for petrogenetic studies. The samples have a narrow SiO_2 range of 65.97–71.05%, with $K_2O + Na_2O$ contents of 5.63–7.00%, indicating a granodiorite composition (Figure 3(b)). The contents of Al_2O_3, CaO, and Na_2O are 14.10–16.29%, 0.37–1.43%, and 2.16–2.55%, respectively, and the ratios of A/CNK and A/NK range from 1.43 to 1.83 and from 1.80 to 2.13, respectively. In the A/NK *versus* A/CNK diagram, all the Getengling pluton samples plot in the S-type granite field (Figure 7(a)) and are strongly peraluminous. The K_2O contents vary between 3.41% and 4.44%, indicating that the Getengling pluton belongs to the high-K calc-alkaline series (Figure 7(b)). Mafic components ($TiO_2 + Fe_2O_3$ + MgO) of the Getengling pluton samples are relatively high, accounting for 6.46–7.62% of the rocks.

All the Getengling pluton samples show light rare earth elements (LREE) enrichment (Figure 8(a)), negative Eu anomalies (δEu = 0.44–0.53), and no obvious Ce anomalies (δCe = 0.98–1.07). In the primitive mantle-normalized spidergram (Figure 8(b)), the Getengling pluton shows enrichment in Pb and large ion lithophile elements such as Rb and Ba and depletion in Sr and high field strength elements such as Nb, Ta, and Ti. The zircon saturation temperature calculated with the method of Watson and Harrison (1983) ranges from

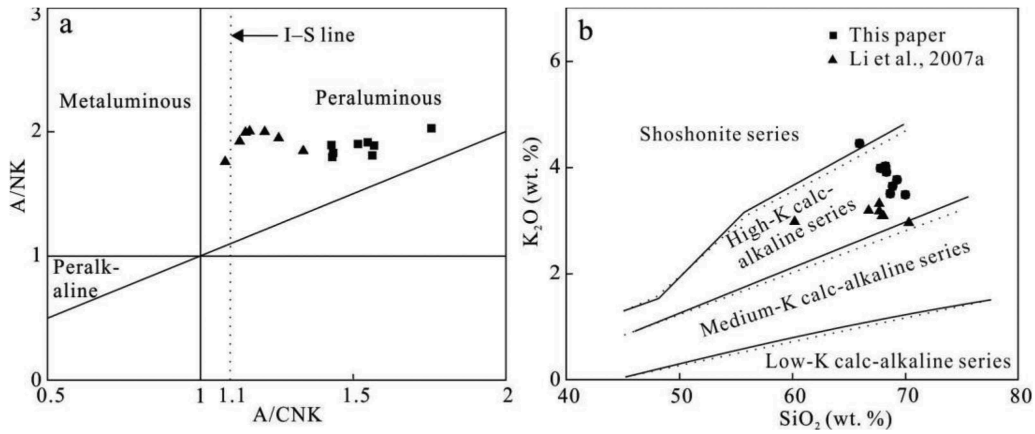

Figure 7. (a) A/NK *versus* A/CNK (modified after Maniar and Piccoil, 1989) and (b) K_2O *versus* SiO_2 diagrams for the Getengling pluton (Morrison 1980).

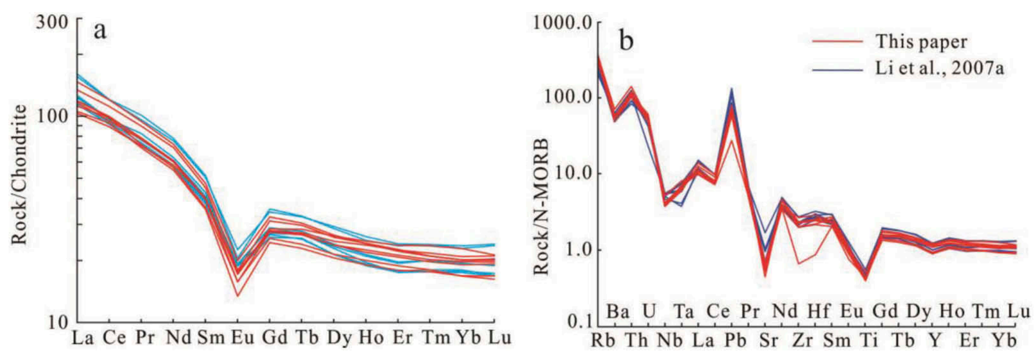

Figure 8. (a) Chondrite-normalized REE patterns (Sun and McDonough 1989) and (b) N-MORB-normalized trace element spidergrams (Sun and McDonough 1989) for the Getengling intrusion.

718 to 838°C with an average of 810°C (Supplementary Table 3).

4.4. Whole-rock Nd isotopes

Sm–Nd isotopic data for the Getengling pluton are presented in Supplementary Table 4. The samples have a narrow range of $^{147}Sm/^{144}Nd$ ratios (0.124–0.130) and $^{143}Nd/^{144}Nd$ ratios (0.512070–0.512102). Calculated $\varepsilon_{Nd}(t)$ values are −2.8 to −3.4 at t = 845 Ma. The calculated two-stage Nd model ages (T_{DM2}) cluster at 1.78–1.75 Ga.

5. Discussion

As mentioned in Section 1, two different viewpoints have been proposed regarding the timing of the collision between the Yangtze and Cathaysia blocks to form the South China Block, i.e. ca. 1100–900 Ma (Grenville orogeny) (Li *et al*. 1999, 2007b, 2008c; Ye *et al*. 2007; Yang *et al*. 2016; Lyu *et al*. 2017) *versus* ca. 860–820 Ma (Zhou *et al*. 2009; Zhao and Cawood 2012; Yao *et al*. 2014a, 2015). One of the key differences between the two hypotheses lies in the genesis of the ca. 850–820-Ma S-type granites, with the former proposing a mantle plume origin and linking them with coeval mafic rocks in Australia (Ye *et al*. 2007; Li *et al*. 2007b, 2008a, 2008c; Huang *et al*. 2015) and the other attributing the formation of these granitoids to continental collision between the Yangtze and Cathaysia blocks (Zhou *et al*. 2009; Wang *et al*. 2012c, 2014; Yao *et al*. 2015). The new geochronological and geochemical data of the Getengling pluton obtained in this study confirm the S-type nature of the magma and support the notion that the collision between the Yangtze and Cathaysia blocks took place at ca. 860–820 Ma. The high CaO/Na_2O ratios and two-stage Nd model ages (1.78–1.75 Ga) support a psammitic sedimentary source (Patino Douce and Harris 1998; Sylvester 1998) for the Getengling magma, possibly caused by crustal thickening in relation to the collision.

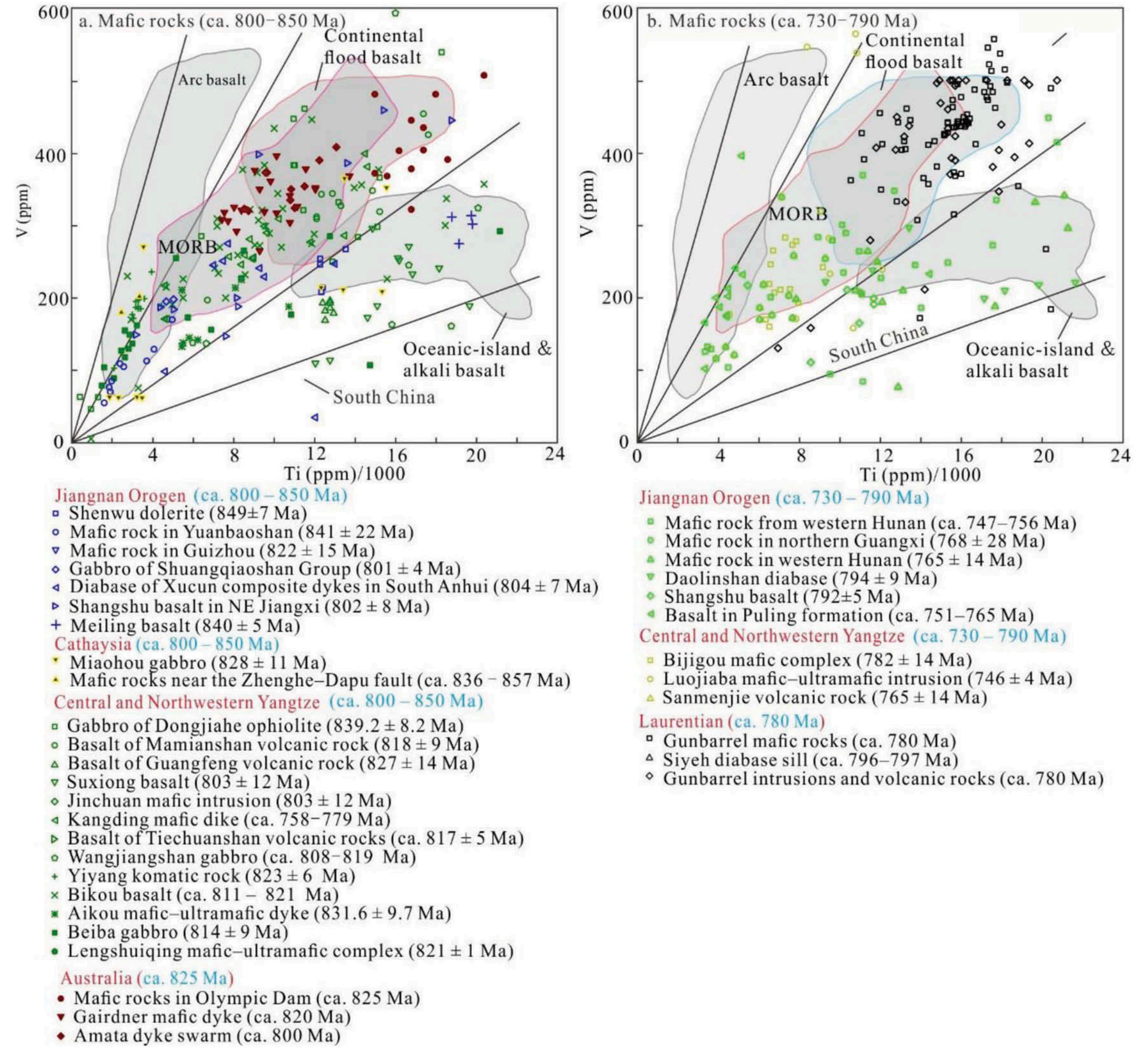

Figure 9. Geochemical discrimination diagrams of Th–Hf–Ta of Wood (1980) for the (a) ca. 800–850-Ma mafic rocks in South China and ca. 820-Ma Gairdner–Amata dike swarms in Australia, and (b) ca. 730–790-Ma mafic rocks in South China and ca. 780-Ma Gunbarrel mafic rocks in western Laurentia. See Supplementary Table 5 for the data resources.

However, as introduced earlier, the data of one intrusion alone cannot convincingly rule out the possibility of a mantle-plume origin for the S-type granites and Proterozoic tectonic evolution of the Jiangnan Orogen. Therefore, the tectonic significance of the geochronological and geochemical data of the Getengling pluton is discussed in context of compilation of the geochronological and geochemical data of Proterozoic rocks in South China, Laurentia, and Australia, as shown in Figures 9–11. Based on general trends revealed by this regional database, we argue that the Getengling pluton, like other ca. 850–820 Ma granitoids in the Jiangnan Orogen, was formed during the collision between the Yangtze and Cathaysia blocks, rather than during rifting of a previously (Grenvillian) formed united South China Block. The detailed reasoning and significance for the tectonic evolution of the Jiangnan Orogen and South China block are discussed below.

First of all, combined with the previously reported ca. 835–820 Ma granitoids (Li *et al*. 2003a; Wang *et al*. 2006, 2013b; Zheng *et al*. 2008; Zhao *et al*. 2011), the zircon LA-ICP-MS U–Pb age of 845 ± 4 Ma obtained in this study for the Getengling pluton suggests that the magmatic activities lasted for 25 Ma. This time interval is much longer than those of felsic magmatism induced by mantle plume activity, which are commonly <5 Ma (Lightfoot *et al*. 1993; Chesley and Ruiz, 1998; Xu *et al*. 2013). Although the high mafic contents ($TiO_2 + Fe_2O_3 + MgO$ = 6.46–7.62%), positive $\varepsilon_{Hf}(t)$, and slight negative $\varepsilon_{Nd}(t)$ values suggest involvement of mantle-derived components, these features are likely caused by remelting of juvenile crust generated by arc

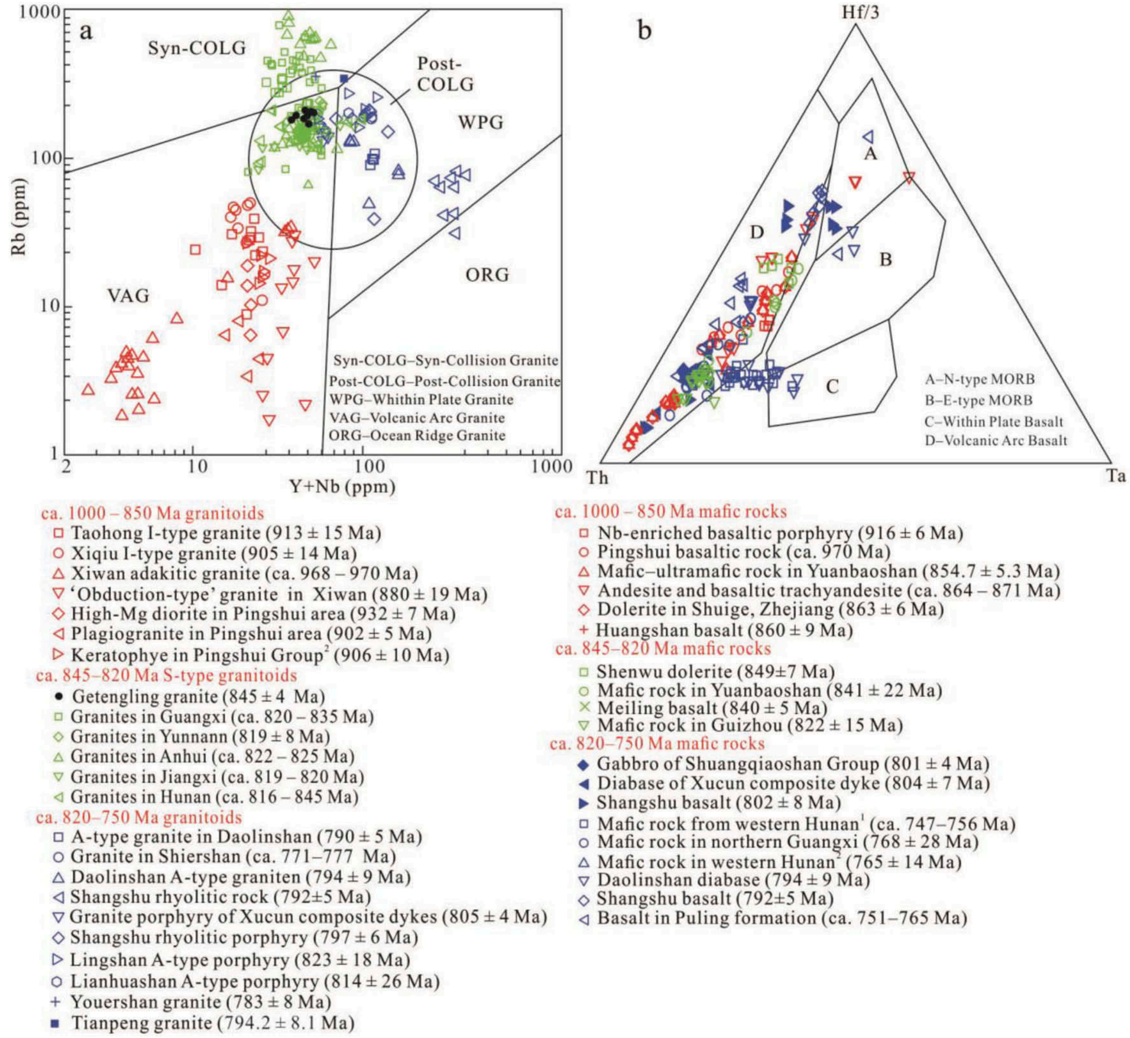

Figure 10. Geochemical discrimination diagrams of (a) Rb – Y + Nb of Pearce *et al.* (1996) for the Proterozoic granitic intrusions and (b) Th – Hf – Ta of Wood (1980) for the mafic rocks in the Jiangnan Orogen. See Supplementary Table 5 for the data resources.

magmatic activities, as proposed by Wu *et al.* (2006a) for other S-type granites in the Jiangnan Orogen. Furthermore, A- and I-type granites, rather than S-type granite, are typically related to mantle plume actives (Hamilton *et al.* 1998; Hames *et al.* 2000; Wang *et al.* 2006; Xu *et al.* 2013).

Second, different from the felsic-dominated magmatism in South China, the ca. 825 and ca. 780-Ma igneous rocks in Australia and west Laurentia are mainly mafic (Downes *et al.* 2006; Wang *et al.* 2006, 2010a; Sandeman et al, 2007; Mackinder, 2014; Huang *et al.* 2015). No ca. 780 Ma felsic rocks were reported in western Laurentia, and the minor ca. 820-Ma granitoids were A type (Preiss *et al.* 2008), different from those in South China. Moreover, the ca. 825 and ca. 780-Ma mafic rocks in Australia and western Laurentia mostly plot in the field of continental flood basalt, which is typically related to mantle plumes (Figure 9). However, the data of the mafic rocks in South China are scattered, with only few located in the field of continental flood basalt, suggesting that the ca. 850–730-Ma mafic rocks in South China were not generated by the Neoproterozoic mantle plume activities.

Third, petrochemical characteristics of granitic rocks of different ages from the Jiangnan Orogen suggest an evolution from magmatic arc through collisional to within-plate environments, the timing of which does not fit the model of 1100–900 Ma collision and the mantle plume peaking at ca. 825 Ma. Different from the subduction-related pre-850 Ma granitoids, the Getengling granitoid and all the other ca. 835–820 Ma S-type granites in the Jiangnan Orogen have Y + Nb and Rb values similar to the syn- and post-collisional granitoids (Figure 10(a)), implying that the tectonic setting in the Jiangnan Orogen changed from plate subduction to continental collision at ca. 850 Ma. The pre-850-Ma plate subduction processes is further demonstrated by the ca. 970–968-Ma Xiwan adakitic granitoid

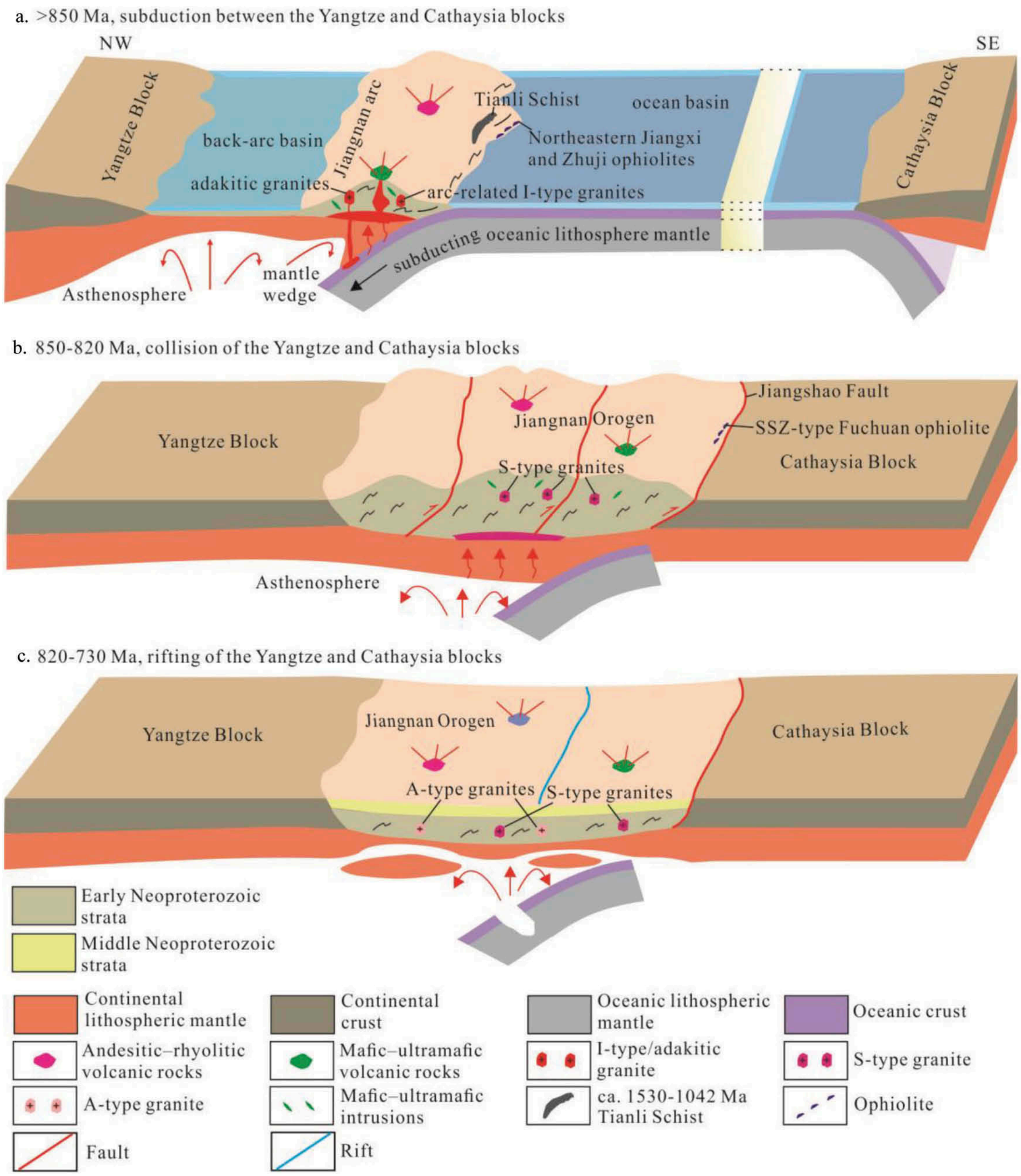

Figure 11. Schematic diagram for the tectonic evolution of the Jiangnan Orogen.

(Li 2003; Gao *et al.* 2009), the 932 ± 7-Ma high-Mg diorite bearing similarities with adakitic andesite, the 916 ± 6-Ma Nb-enriched basaltic porphyry (Chen *et al.* 2009a), and other ca. 950–850 Ma mafic–felsic magmatic rocks (Shu *et al.* 2006; Ye *et al.* 2007; Li *et al.* 2008a, 2009; Chen *et al.* 2009a; Yao *et al.* 2014b, 2015).

In addition, the pre-820-Ma bimodal volcanic rocks in South China could be generated under local extensional tectonic setting during the collision in the Jiangnan Orogen and the subduction in northern and southwestern Yangtze (Li *et al.* 2002; Ling *et al.* 2003; Lyu *et al.* 2017). The lower unites of the Neoproterozoic strata could be the clastic sources for the upper unites, resulting in the similar sedimentary provenances between the two sets of strata as indicated by Yang *et al.* (2015). Consequently, the ca. 825–815-Ma angular unconformity between the two Neoproterozoic successions in the Jiangnan Orogen, as constrained from ages of the volcanic rocks in the upper and lower units, is also likely to be generated by the collision.

In contrast, the post-820-Ma igneous rocks in the Jiangnan Orogen include a series of A- and S-type granites, bimodal volcanic rocks, and other rift-related volcanic-intrusive rocks; most granite and some basalt samples plot in the intra-plate granite and basalt fields (Figure 10(a,b)). This suggests that the Jiangnan Orogen stepped into the post-collisional stage after ca. 820 Ma, likely related to the re-splitting between the Yangtze and Cathaysia blocks (Li *et al*. 2008c; Zhao and Cawood 2012; Wang *et al*. 2012b), or a failed intracontinental rift between the Yangtze and Cathaysia blocks (Li *et al*. 2008c).

In view of the above arguments, the Proterozoic tectonic evolution of the Jiangnan Orogen is outlined as follows (Figure 11). (A) The subduction resulted in a series of metamorphic and mafic–felsic magmatic activities before ca. 850 Ma. (B) The collision between the Yangtze and Cathaysia blocks may have occurred at ca. 850–820 Ma, generating the unconformity between the early and middle Neoproterozoic strata, widespread mafic–felsic volcanic rocks, S-type granites, and associated mafic intrusions. (C) The post-820-Ma intracontinental rifting led to the breakup between the Yangtze and Cathaysia blocks, forming S- and A-type granites, bimodal volcanic rocks, and other mafic–felsic rocks.

6. Conclusions

(1) The Getengling granitoid with the zircon LA-ICP-MS U–Pb age of 845 ± 4 Ma is one of the Neoproterozoic S-type granites in the Jiangnan Orogen. Both ancient crustal sediments and juvenile mantle-derived components generated by precursor arc magmatic activities may have served as the magma source for the pluton.
(2) Both the ca. 850–730-Ma granitoids and mafic rocks in South China are geochemically different from the coeval large igneous provinces in Australia and western Laurentia, suggesting that they are not generated by mantle plume activities.
(3) The geochemical characteristics of the pre-850-Ma, ca. 850–820-Ma, and post-820-Ma igneous rocks in the Jiangnan Orogen suggest a tectonic evolution from plate subduction-related magmatic arcs, through collision between the Yangtze and Cathaysia blocks, to post-collisional extensional environment.
(4) The collision between the Yangtze and Cathaysian blocks to form the South China block took place at ca. 850–820 Ma, rather than during the ca. 1100–900-Ma Grenville orogeny.

Acknowledgements

The paper was financially co-supported the DREAM project of MOST, China: [Grant Number 2016YFC0600401], the National Natural Science Foundation of China: Grant Numbers 41472171, 41672077, and 41302049], and the Bureau of China Geological Survey: [Grant Number 12120113067100]. We gratefully acknowledge the careful and constructive comments of Dr. Robert J. Stern and two anonymous reviewers, which considerably improved the manuscript. We are thankful for the assistance from Congying Li for the zircon U–Pb dating and Le Zhang and Jinlong Ma for the zircon Hf and whole-rock Sr–Nd isotope analyses. A particular thank is given to Guojun Dong and Juntao Ning from Hunan Bureau of Geology and Mineral Exploration for their help in the field investigation.

Disclosure statement

No potential conflict of interest was reported by the authors.

Funding

The paper was financially co-supported the DREAM project of MOST, China: [Grant Number 2016YFC0600401], the National Natural Science Foundation of China: Grant Numbers [41472171], [41672077], and [41302049], and the Bureau of China Geological Survey: [Grant Number 12120113067100].

Highlights

(1) Getengling pluton being S-type granite with certain I-type granite affinities.
(2) Getengling pluton forming at 845 ± 4 Ma.
(3) Mafic and felsic rocks in South China being different from those in Australia and western Laurentia.

Compositions of the granites in Jiangnan Orogen suggesting the Yangtze and Cathaysia collided at ca. 850 Ma.

ORCID

Yuhua Zhu http://orcid.org/0000-0002-7879-9153

References

Black, L.P., Kamo, S.L., Allen, C.M., Aleinikoff, J.N., Davis, D.W., Korsch, R.J., and Foudoulis, C., 2003, TEMORA 1: A new zircon standard for Phanerozoic U–Pb geochronology: Chemical Geology, v. 200, p. 155–170. doi:10.1016/S0009-2541(03)00165-7

Cawood, P., Zhao, G., Yao, J., Wang, W., Xu, Y., and Wang, Y., 2017, Reconstructing South China in Phanerozoic and Precambrian supercontinents: Earth-Science Reviews. doi:10.1016/j.earscirev.2017.06.001

Chen, H., Ni, P., Chen, R., Lv, Z., Pang, Z., Wang, G., and Yuan, H., 2016, Chronology and geological significance of spilite–Keratophyre in Pingshui Formation, northwest Zhejiang Province: Geology in China, v. 43, p. 400–418. [in Chinese with English abstract.]

Chen, J., Ka, F., Xing, F., Xu, X., and Zhou, T., 1991, Magmatism along the southeast margin of the Yangtze block: Precambrian collision of the Yangtze and Cathysia blocks of China: Geology, v. 19, p. 815–818. doi:10.1130/0091-7613(1991)019<0815:MATSMO>2.3.CO;2

Chen, Z., Guo, K., Dong, Y., Chen, R., Li, L., Liang, Y., Li, C., Yu, X., Zhao, L., and Xing, G., 2009a, Possible early Neoproterozoic magmatism associated with slab window in the Pingshui segment of the Jiangshan–Shaoxing suture zone: Evidence from zircon LA-ICP-MS U–Pb geochronology and geochemistry: Science in China Series D: Earth Sciences, v. 52, p. 925–939. doi:10.1007/s11430-009-0071-6

Chen, Z., Xing, G., Guo, K., Dong, Y., Chen, R., Zeng, Y., Li, L., He, Z., and Zhao, L., 2009b, Petrogenesis of the Pingshui keratophyre from Zhejiang: Zircon U–Pb age and Hf isotope constraints: Chinese Science Bulletin, v. 54, p. 610–617. [in Chinese with English abstract.]

Chesley, J.T., and Ruiz, J., 1998, Crust–Mantle interaction in large igneous provinces: Implications from the Re–Os isotope systematics of the Columbia River flood basalts: Earth and Planetary Science Letters, v. 154, p. 1–11. doi:10.1016/S0012-821X(97)00176-3

Ding, B., Shi, R., Zhi, X., Zheng, L., and Chen, L., 2008, Neoproterozoic (□ 850 Ma) subduction in the Jiangnan orogen: Evidence from the SHRIMP U–Pb dating of the SSZ-type ophiolite in southern Anhui Province: Acta Petrologica Et Mineralogica, v. 27, p. 375–388. [in Chinese with English abstract.]

Downes, P., Wartho, J., and Griffin, B., 2006, Magmatic evolution and ascent history of the Aries micaceous kimberlite, Central Kimberley Basin, Western Australia: Evidence from zoned phlogopite phenocrysts, and UV laser 40Ar/39Ar analysis of phlogopite–biotite: Journal of Petrology, v. 47, p. 1751–1783. doi:10.1093/petrology/egl026

Gao, J., Klemd, R., Long, L., Xiong, X., and Qian, Q., 2009, Adakitic signature formed by fractional crystallization: An interpretation for the Neo–Proterozoic meta–plagiogranites of the NE Jiangxi ophiolitic mélange belt, South China: Lithos, v. 110, p. 277–293. doi:10.1016/j.lithos.2009.01.009

Gao, L., Chen, J., Ding, X., Liu, Y., Zhang, C., Zhang, H., Liu, Y., Pang, W., and Zhang, Y., 2011, Zircon SHRIMP U–Pb dating of the tuff bed of Lengjiaxi and Banxi groups, northeastern Hunan: constraints on the Wuling Movement: Geological Bulletin of China, v. 30, p. 1001–1008. [in Chinese with English abstract.]

Gao, L., Dai, C., Liu, Y., Wang, M., Wang, X., Chen, J., and Ding, X., 2010a, Zircon SHRIMP U–Pb dating of the tuffaceous bed of Xiajiang Group in Guizhou Province and its stratigraphic implication: Geology in China, v. 37, p. 1071–1080. [in Chinese with English abstract.]

Gao, L., Dai, C., Liu, Y., Wang, M., Wang, X., Chen, J., Ding, X., Zhang, C., Cao, Q., and Liu, J., 2010b, Zircon SHRIMP U–Pb dating of tuff bed of the Sibao Group in Southeastern Guizhou–northern Guangxi area, China and its stratigraphic implication: Geological Bulletin of China, v. 29, p. 1259–1267. [in Chinese with English abstract.]

Ge, W., Li, X., Li, Z., and Zhou, H., 2001, Mafic intrusions in Longsheng area: Age and its geological implications: Chinese Journal of Geology, v. 36, p. 112–118. [in Chinese with English abstract.]

Hames, W., Renne, P., and Ruppel, C., 2000, New evidence for geologically instantaneous emplacement of earliest Jurassic Central Atlantic magmatic province basalts on the North American margin: Geology, v. 28, p. 859–862. doi:10.1130/0091-7613(2000)28<859:NEFGIE>2.0.CO;2

Hamilton, M., Pearson, D., Thompson, R., Kelley, S., and Emeleus, C., 1998, Rapid eruption of Skye lavas inferred from precise U–Pb and Ar–Ar dating of the Rum and Cuillin plutonic complexes: Nature, v. 394, p. 260–263. doi:10.1038/28361

HNBGMR (Bureau of geology and mineral Resource of Hunan province), 1988, Regional geology of Hunan province: Beijing, Geological Publishing House, 722 p. [in Chinese.]

Huang, Q., Kamenetsky, V.S., McPhie, J., Ehrig, K., Meffre, S., Maas, R., Thompson, J., Kamenetsky, M., Chambefort, I., and Apukhtina, O., 2015, Neoproterozoic (ca. 820–830Ma) mafic dykes at Olympic Dam, South Australia: Links with the Gairdner Large Igneous Province: Precambrian Research, v. 271, p. 160–172. doi:10.1016/j.precamres.2015.10.001

Li, C., Zhang, H., Wang, F., Liu, J., Sun, Y., Hao, X., Li, Y., and Sun, W., 2012, The formation of the Dabaoshan porphyry molybdenum deposit induced by slab rollback: Lithos, v. 150, p. 101–110. doi:10.1016/j.lithos.2012.04.001

Li, L., Lin, S., Xing, G., Davis, D.W., Davis, W.J., Xiao, W., and Yin, C., 2013, Geochronology and geochemistry of volcanic rocks from the Shaojiwa Formation and Xingzi Group, Lushan area, SE China: Implications for Neoproterozoic back-arc basin in the Yangtze Block: Precambrian Research, v. 238, p. 1–17. doi:10.1016/j.precamres.2013.09.016

Li, P., Chen, G., Xu, D., He, Z., and Fu, G., 2007a, Petrological and geochemical characteristics and petrogenesis of Neoproterozoic peraluminous granites in Northeastern Hunan Province: Geotectonica Et Metallogenia, v. 31, p. 126–136. [in Chinese with English abstract.]

Li, W., 2003, Adakitic granites within the NE Jiangxi ophiolites, South China: Geochemical and Nd isotopic evidence: Precambrian Research, v. 122, p. 29–44. doi:10.1016/S0301-9268(02)00206-1

Li, W., Li, X., and Li, Z., 2005a, Neoproterozoic bimodal magmatism in the Cathaysia Block of South China and its tectonic significance: Precambrian Research, v. 136, p. 51–66. doi:10.1016/j.precamres.2004.09.008

Li, W., Li, X., and Li, Z., 2008a, Middle Neoproterozoic syn–Rifting volcanic rocks in Guangfeng, South China: Petrogenesis and tectonic significance: Geological Magazine, v. 145, p. 475–489. doi:10.1017/S0016756808004561

Li, W., Li, X., Li, Z., and Lou, F., 2008a, Obduction–Type granites within the NE Jiangxi Ophiolite: Implications for the final amalgamation between the Yangtze and Cathaysia Blocks: Gondwana Research, v. 13, p. 288–301. doi:10.1016/j.gr.2007.12.010

Li, W., Li, X., and Li, Z.-X., 2010b, Ca. 850 Ma bimodal volcanic rocks in northeastern Jiangxi Province, South China: Initial extension during the breakup of Rodinia?: American Journal of Science, v. 310, p. 951–980. doi:10.2475/09.2010.08

Li, X., 1999, U–Pb zircon ages of granites from the southern margin of the Yangtze Block: timing of Neoproterozoic Jinning: Orogeny in SE China and implications for Rodinia Assembly: Precambrian Research, v. 97, p. 43–57. doi:10.1016/S0301-9268(99)00020-0

Li, X., Li, W., Li, Z., and Liu, Y., 2008b, 850–790 Ma bimodal volcanic and intrusive rocks in northern Zhejiang, South China: A major episode of continental rift magmatism during the breakup of Rodinia: Lithos, v. 102, p. 341–357. doi:10.1016/j.lithos.2007.04.007

Li, X., Li, W., Li, Z., Lo, C., Wang, J., Ye, M., and Yang, Y., 2009, Amalgamation between the Yangtze and Cathaysia Blocks in South China: Constraints from SHRIMP U–Pb zircon ages, geochemistry and Nd–Hf isotopes of the Shuangxiwu volcanic rocks: Precambrian Research, v. 174, p. 117–128. doi:10.1016/j.precamres.2009.07.004

Li, X., Li, Z., Ge, W., Zhou, H., Li, W., Liu, Y., and Wingate, M.T., 2003a, Neoproterozoic granitoids in South China: Crustal melting above a mantle plume at ca: 825 Ma? Precambrian Research, v. 122, p. 45–83. doi:10.1016/S0301-9268(02)00207-3

Li, X., Li, Z., Zhou, H., Liu, Y., and Kinny, P.D., 2002, U–Pb zircon geochronology, geochemistry and Nd isotopic study of Neoproterozoic bimodal volcanic rocks in the Kangdian Rift of South China: Implications for the initial rifting of Rodinia: Precambrian Research, v. 113, p. 135–154. doi:10.1016/S0301-9268(01)00207-8

Li, X., Li, Z., Zhou, H., Liu, Y., Liang, X., and Li, W., 2003b, SHRIMP U–Pb zircon age, geochemistry and Nd isotope of the Guandaoshan pluton in SW Sichuan: Petrogenesis and tectonic significance: Science in China Series D: Earth Sciences, v. 46, p. 73–83.

Li, X., Long, W., Li, Q., Liu, Y., Zheng, Y., Yang, Y., Chamberlain, K.R., Wan, D.F., Guo, C.H., and Wang, X., 2010a, Penglai zircon megacrysts: A potential new working reference material for microbeam determination of Hf–O isotopes and U–Pb age: Geostandards and Geoanalytical Research, v. 34, p. 117–134. doi:10.1111/j.1751-908X.2010.00036.x

Li, X., Qi, C., Liu, Y., Liang, X., Tu, X., Xie, L., and Yang, Y., 2005b, Petrogenesis of the Neoproterozoic bimodal volcanic rocks along the western margin of the Yangtze Block: New constraints from Hf isotopes and Fe/Mn ratios: Chinese Science Bulletin, v. 50, p. 2481–2486. doi:10.1360/982005-287

Li, X., Zhou, G., Jianxin, Z., Fanning, C., and Compston, W., 1994, SHRIMP ion microprobe zircon U–Pb age and Sm–Nd isotopic characteristics of the NE Jiangxi ophiolite and its tectonic implications: Chinese Journal of Geochemistry, v. 13, p. 317–325. doi:10.1007/BF02838521

Li, X.-H., Li, Z.-X., Sinclair, J.A., Li, W.-X., and Carter, G., 2006, Revisiting the "Yanbian Terrane": Implications for Neoproterozoic tectonic evolution of the western Yangtze Block, South China: Precambrian Research, v. 151, p. 14–30. doi:10.1016/j.precamres.2006.07.009

Li, Z., Bogdanova, S., Collins, A., Davidson, A., De Waele, B., Ernst, R., Fitzsimons, I., Fuck, R., Gladkochub, D., and Jacobs, J., 2008c, Assembly, configuration, and break–Up history of Rodinia: A synthesis: Precambrian Research, v. 160, p. 179–210. doi:10.1016/j.precamres.2007.04.021

Li, Z., Li, X., Kinny, P., and Wang, J., 1999, The breakup of Rodinia: Did it start with a mantle plume beneath South China?: Earth and Planetary Science Letters, v. 173, p. 171–181. doi:10.1016/S0012-821X(99)00240-X

Li, Z., Li, X., Kinny, P., Wang, J., Zhang, S., and Zhou, H., 2003b, Geochronology of Neoproterozoic syn-rift magmatism in the Yangtze Craton, South China and correlations with other continents: Evidence for a mantle superplume that broke up Rodinia: Precambrian Research, v. 122, p. 85–109. doi:10.1016/S0301-9268(02)00208-5

Li, Z., Wartho, J.A., Occhipinti, S., Zhang, C., Li, X., Wang, J., and Bao, C., 2007b, Early history of the eastern Sibao Orogen (South China) during the assembly of Rodinia: New mica Ar^{40}/Ar^{39} dating and SHRIMP U–Pb detrital zircon provenance constraints: Precambrian Research, v. 159, p. 79–94. doi:10.1016/j.precamres.2007.05.003

Liang, X., Wei, G., Li, X., and Liu, Y., 2003, Precise measurement of 143Nd/144Nd and Sm/Nd ratios using multiple–Collectors inductively coupled plasma–Mass spectrometer (MC-ICP-MS): Geochimica, v. 32, p. 91–96.

Lightfoot, P., Hawkesworth, C., Hergt, J., Naldrett, A., Gorbachev, N., Fedorenko, V., and Doherty, W., 1993, Remobilisation of the continental lithosphere by a mantle plume: Major-, trace-element, and Sr-, Nd-, and Pb- isotope evidence from picritic and tholeiitic lavas of the Noril'sk District, Siberian Trap, Russia: Contributions to Mineralogy and Petrology, v. 114, p. 171–188. doi:10.1007/BF00307754

Ling, W., Gao, S., Zhang, B., Li, H., Liu, Y., and Cheng, J., 2003, Neoproterozoic tectonic evolution of the northwestern Yangtze craton, South China: Implications for amalgamation and break–Up of the Rodinia Supercontinent: Precambrian Research, v. 122, p. 111–140. doi:10.1016/S0301-9268(02)00222-X

Liu, Y., Gao, S., Hu, Z., Gao, C., Zong, K., and Wang, D., 2010a, Continental and oceanic crust recycling-induced melt-peridotite interactions in the Trans-North China Orogen: U–Pb dating, Hf isotopes and trace elements in zircons from mantle xenoliths: Journal of Petrology, v. 51, p. 537–571. doi:10.1093/petrology/egp082

Liu, Y., Hu, Z., Zong, K., Gao, C., Gao, S., Xu, J., and Chen, H., 2010b, Reappraisement and refinement of zircon U–Pb isotope and trace element analyses by LA-ICP-MS: Chinese Science Bulletin, v. 55, p. 1535–1546. doi:10.1007/s11434-010-3052-4

Liu, Y., Liu, H., and Li, X., 1996, Simultaneous and precise determination of 40 trace elements in rock samples using ICP-MS: Geochimica, v. 25, p. 552–558.

Ludwig, K., 2004, Users manual for ISOPLOT/EX, version3. 1. A geochronological toolkit for Microsoft Excel Berkeley Geochronology Center: Special Publication 4.

Lyu, P.-L., Li, W.-X., Wang, X.-C., Pang, C.-J., Cheng, J.-X., and Li, X.-H., 2017, Initial breakup of supercontinent Rodinia as recorded by ca 860–840Ma bimodal volcanism along the southeastern margin of the Yangtze Block, South China: Precambrian Research, v. 296, p. 148–167. doi:10.1016/j.precamres.2017.04.039

Ma, T., Chen, L., Bai, D., Zhou, K., Li, G., and Wang, X., 2009, Zircon shrimp dating and geochemical characteristics of

Neoproterozoic granites in southeastern Hunan: Geology in China, v. 36, p. 65–73. [in Chinese with English abstract.]

Ma, X., Yang, K., Li, X., Dai, C., Zhang, H., and Zhou, Q., 2016, Neoproterozoic Jiangnan Orogeny in southeast Guizhou, South China: Evidence from U–Pb ages for detrital zircons from the Sibao Group and Xiajiang Group: Canadian Journal of Earth Sciences, v. 53, p. 219–230. doi:10.1139/cjes-2015-0052

Mackinder, A., 2014, A petrographic, geochemical and isotopic study of the 780 Ma Gunbarrel Large Igneous Province, western North America [Master degree]: Carleton University, 1–127 p.

Maniar, P.D., and Piccoli, P.M., 1989, Tectonic discrimination of granitoids: Geological Society of America Bulletin, v. 101, p. 635–643. doi:10.1130/0016-7606(1989)101<0635:TDOG>2.3.CO;2

Middlemost, E.A.K., 1994, Naming materials in the magma igneous rock system: Earth-Science Reviews, v. 37, p. 215–224. doi:10.1016/0012-8252(94)90029-9

Morrison, G.W., 1980, Characteristics and tectonic setting of the shoshonite rock association: Lithos, v. 13, p. 97–108. doi:10.1016/0024-4937(80)90067-5

Patino Douce, A.E., and Harris, N., 1998, Experimental constraints on Himalayan anatexis: Journal of Petrology, v. 39, p. 689–710. doi:10.1093/petroj/39.4.689

Pearce, J.A., 1996, Sources and settings of granitic rocks: Episodes, v. 19, p. 120–125.

Preiss, W.V., Fanning, C.M., Szpunar, M.A., and Burtt, A., 2008, Age and tectonic significance of the Mount Crawford granite gneiss and a related intrusive in the Oakbank inlier, Mount Lofty Ranges, South Australia: MESA Journal, v. 49, p. 38–49.

Sandeman, H., Ootes, L., and Jackson, V., 2007, Field petrographic, and petrochemical data for the Faber Sill: Insights into the petrogenesis of a Gunbarrel event intrusion in the Wopmay Orogen. NWT, Canada: Northwest Territories Geoscience Office, NWT Open File Report. 7, 25.

Sandeman, H.A., Ootes, L., Cousens, B., and Kilian, T., 2014, Petrogenesis of Gunbarrel magmatic rocks: Homogeneous continental tholeiites associated with extension and rifting of Neoproterozoic Laurentia: Precambrian Research, v. 252, p. 166–179. doi:10.1016/j.precamres.2014.07.007

Shu, L., Faure, M., Jiang, S., Yang, Q., and Wang, Y., 2006, SHRIMP zircon U–Pb age, litho–and biostratigraphic analyses of the Huaiyu Domain in South China: Episodes, v. 29, p. 244–252.

Shu, L., Zhou, G., Shi, Y., and Yin, J., 1994, Study of the high pressure metamorphic blueschist and its Late Proterozoic age in the eastern Jiangnan belt: Chinese Science Bulletin, v. 39, p. 1200–1204.

Sun, S., and McDonough, W., 1989, Chemical and isotopic systematics of oceanic basalts: Implications for mantle composition and processes: Geological Society, London, Special Publications, v. 42, p. 313–345. doi:10.1144/GSL.SP.1989.042.01.19

Sylvester, P.J., 1998, Post-collisional strongly peraluminous granites: Lithos, v. 45, p. 29–44. doi:10.1016/S0024-4937(98)00024-3

Tu, X., Zhang, H., Deng, W., Ling, M., Liang, H., Liu, Y., and Sun, W., 2011, Application of RESOlution in-situ laser ablation ICP-MS in trace element analyses: Geochimica, v. 40, p. 83–98.

Wan, Y., Liu, D., Xu, M., Zhuang, J., Song, B., Shi, Y., and Du, L., 2007, SHRIMP U–Pb zircon geochronology and geochemistry of metavolcanic and metasedimentary rocks in Northwestern Fujian, Cathaysia block, China: tectonic implications and the need to redefine lithostratigraphic units: Gondwana Research, v. 12, p. 166–183. doi:10.1016/j.gr.2006.10.016

Wang, J., Li, X., Duan, T., Liu, D., Song, B., Li, Z., and Gao, Y., 2003, Zircon SHRIMP U–Pb dating for the Cangshuipu volcanic rocks and its implications for the lower boundary age of the Nanhua strata in South China: Chinese Science Bulletin, v. 48, p. 1663–1669. doi:10.1360/03wd0168

Wang, J., Zhou, X., Deng, Q., Fu, X., Duan, T., and Guo, X., 2015, Sedimentary successions and the onset of the Neoproterozoic Jiangnan sub-basin in the Nanhua rift, South China: International Journal of Earth Sciences, v. 104, p. 521–539. doi:10.1007/s00531-014-1107-5

Wang, M., Dai, C.G., Wang, X., Chen, J.S., and Ma, H., 2011a, In situ zircon geochronology and Hf isotope of muscovite bearing leucogranites from Fanjingshan, Guizhou Province, and constraints on continental growth of the Southern China block: Earth Science Frontiers, v. 18, p. 213–223. [in Chinese with English abstract.]

Wang, Q., Wyman, D.A., Li, Z.-X., Bao, Z.-W., Zhao, Z.-H., Wang, Y.-X., Jian, P., Yang, Y.-H., and Chen, -L.-L., 2010a, Petrology, geochronology and geochemistry of ca. 780Ma A-type granites in South China: Petrogenesis and implications for crustal growth during the breakup of the supercontinent Rodinia: Precambrian Research, v. 178, p. 185–208. doi:10.1016/j.precamres.2010.02.004

Wang, W., Zhou, M., Yan, D., and Li, J., 2012a, Depositional age, provenance, and tectonic setting of the Neoproterozoic Sibao Group, southeastern Yangtze Block, South China: Precambrian Research, v. 192–195, p. 107–124. doi:10.1016/j.precamres.2011.10.010

Wang, W., Zhou, M., Yan, D., Li, L., and Malpas, J., 2013a, Detrital zircon record of Neoproterozoic active–Margin sedimentation in the eastern Jiangnan Orogen, South China: Precambrian Research, v. 235, p. 1–19. doi:10.1016/j.precamres.2013.05.013

Wang, W., Zhou, M.-F., Zhao, J.-H., Pandit, M.K., Zheng, J.-P., and Liu, Z.-R., 2016, Neoproterozoic active continental margin in the southeastern Yangtze Block of South China: Evidence from the ca. 830–810Ma sedimentary strata: Sedimentary Geology, v. 342, p. 254–267. doi:10.1016/j.sedgeo.2016.07.006

Wang, X., Li, X., Li, W., and Li, Z., 2007a, Ca. 825 Ma komatiitic basalts in South China: First evidence for> 1500 C mantle melts by a Rodinian mantle plume: Geology, v. 35, p. 1103–1106. doi:10.1130/G23878A.1

Wang, X., Li, X., Li, W., Li, Z., Liu, Y., Yang, Y., Liang, X., and Tu, X., 2008a, The Bikou basalts in the northwestern Yangtze block, South China: Remnants of 820–810 Ma continental flood basalts?: Geological Society of America Bulletin, v. 120, p. 1478–1492. doi:10.1130/B26310.1

Wang, X., Li, X., Li, Z., Li, Q., Tang, G., Gao, Y., Zhang, Q., and Liu, Y., 2012b, Episodic Precambrian crust growth: Evidence from U–Pb ages and Hf–O isotopes of zircon in the Nanhua Basin, central South China: Precambrian Research, v. 222–223, p. 386–403. doi:10.1016/j.precamres.2011.06.001

Wang, X., Li, X., Li, Z., Liu, Y., and Yang, Y., 2010b, The Willouran basic province of South Australia: Its relation to the Guibei large igneous province in South China and the breakup of Rodinia: Lithos, v. 119, p. 569–584. doi:10.1016/j.lithos.2010.08.011

Wang, X., Shu, L., Xing, G., Zhou, J., Tang, M., Shu, X., Qi, L., and Hu, Y., 2012c, Post-orogenic extension in the eastern part of the Jiangnan orogen: Evidence from ca 800–760Ma volcanic rocks: Precambrian Research, v. 222–223, p. 404–423. doi:10.1016/j.precamres.2011.07.003

Wang, X., Zhao, G., Zhou, J., Liu, Y., and Hu, J., 2008b, Geochronology and Hf isotopes of zircon from volcanic rocks of the Shuangqiaoshan Group, South China: Implications for the Neoproterozoic tectonic evolution of the eastern Jiangnan orogen: Gondwana Research, v. 14, p. 355–367. doi:10.1016/j.gr.2008.03.001

Wang, X., Zhou, J., Griffin, W.A., Wang, R., Qiu, J.S., O'Reilly, S., Xu, X., Liu, X., and Zhang, G., 2007b, Detrital zircon geochronology of Precambrian basement sequences in the Jiangnan orogen: Dating the assembly of the Yangtze and Cathaysia Blocks: Precambrian Research, v. 159, p. 117–131. doi:10.1016/j.precamres.2007.06.005

Wang, X., Zhou, J., Qiu, J., and Gao, J., 2004, Geochemistry of the Meso- to Neoproterozoic basic–Acid rocks from Hunan Province, South China: Implications for the evolution of the western Jiangnan orogen: Precambrian Research, v. 135, p. 79–103. doi:10.1016/j.precamres.2004.07.006

Wang, X., Zhou, J., Qiu, J., Jiang, S., and Shi, Y., 2008c, Geochronology and geochemistry of Neoproterozoic mafic rocks from western Hunan, South China: Implications for petrogenesis and post-orogenic extension: Geological Magazine, v. 145, p. 215–233. doi:10.1017/S0016756807004025

Wang, X., Zhou, J., Qiu, J., Zhang, W., Liu, X., and Zhang, G., 2006, LA-ICP-MS U–Pb zircon geochronology of the Neoproterozoic igneous rocks from Northern Guangxi, South China: Implications for tectonic evolution: Precambrian Research, v. 145, p. 111–130. doi:10.1016/j.precamres.2005.11.014

Wang, X., Zhou, J., Wan, Y., Kitajima, K., Wang, D., Bonamici, C., Qiu, J.S., and Sun, T., 2013b, Magmatic evolution and crustal recycling for Neoproterozoic strongly peraluminous granitoids from southern China: Hf and O isotopes in zircon: Earth and Planetary Science Letters, v. 366, p. 71–82. doi:10.1016/j.epsl.2013.02.011

Wang, X.-C., Li, Z.-X., Li, X.-H., Li, Q.-L., Tang, G.-Q., Zhang, Q.-R., and Liu, Y., 2011b, Nonglacial origin for low-δ18O Neoproterozoic magmas in the South China Block: Evidence from new in-situ oxygen isotope analyses using SIMS: Geology, v. 39, p. 735–738. doi:10.1130/G31991.1

Wang, Y., Zhang, Y., Fan, W., Geng, H., Zou, H., and Bi, X., 2014, Early Neoproterozoic accretionary assemblage in the Cathaysia Block: Geochronological, Lu–Hf isotopic and geochemical evidence from granitoid gneisses: Precambrian Research, v. 249, p. 144–161. doi:10.1016/j.precamres.2014.05.003

Watson, E.B., and Harrison, T.M., 1983, Zircon saturation revisited: Temperature and composition effects in a variety of crustal magma types: Earth and Planetary Science Letters, v. 64, p. 295–304. doi:10.1016/0012-821X(83)90211-X

Wei, G., Liang, X., Li, X., and Liu, Y., 2002, Precise measurement of Sr isotopic composition of liquid and solid base using (LA) MC-ICPMS: Geochimica, v. 31, p. 295–305.

Wood, D.A., 1980, The application of a Th–Hf–Ta diagram to problems of tectonomagmatic classification and to establishing the nature of crustal contamination of basaltic lavas of the British Tertiary Volcanic Province: Earth and Planetary Science Letters, v. 50, p. 11–30. doi:10.1016/0012-821X(80)90116-8

Wu, F.Y., Yang, Y.H., Xie, L.W., Yang, J.H., and Xu, P., 2006b, Hf isotopic compositions of the standard zircons and baddeleyites used in U-Pb geochronology: Chemical Geology, v. 234, p. 105–126. doi:10.1016/j.chemgeo.2006.05.003

Wu, R., Zheng, Y., and Wu, Y., 2005, Zircon U–Pb age, element and oxygen isotope geochemistry of Neoproterozoic granites at Shiershan in south Anhui Province: Geological Journal of China Universities, v. 11, p. 364–382. [in Chinese with English abstract.]

Wu, R., Zheng, Y., and Wu, Y., 2007, Zircon U–Pb age and isotope geochemistry of Neoproterozoic Jingtan volcanics in South Anhui: Geological Journal of China Universities, v. 13, p. 282–296. [in Chinese with English abstract.]

Wu, R., Zheng, Y., Wu, Y., Zhao, Z.F., Zhang, S., Liu, X., and Wu, F., 2006a, Reworking of juvenile crust: Element and isotope evidence from Neoproterozoic granodiorite in South China: Precambrian Research, v. 146, p. 179–212. doi:10.1016/j.precamres.2006.01.012

Xu, D., Deng, T., Chi, G., Wang, Z., Zou, F., Zhang, J., and Zou, S., 2017, Gold mineralization in the Jiangnan Orogenic Belt of South China: Geological, geochemical and geochronological characteristics, ore deposittype and geodynamic setting: Ore Geology Reviews, v. 88, p. 565–618. doi:10.1016/j.oregeorev.2017.02.004

Xu, D., Gu, X., Li, P., Chen, G., Xia, B., Robert, B., He, Z., and Fu, G., 2007, Mesoproterozoic–Neoproterozoic transition: Geochemistry, provenance and tectonic setting of clastic sedimentary rocks on the SE margin of the Yangtze Block, South China: Journal of Asian Earth Sciences, v. 29, p. 637–650. doi:10.1016/j.jseaes.2006.04.006

Xu, Y., He, B., Luo, Z., and Liu, H., 2013, Study on mantle plume and large igneous provinces in China: An overview and perspectives: Bulletin of Mineralogy, Petrology and Geochemistry, v. 32, p. 25–39. [in Chinese with English abstract.]

Xue, H., Ma, F., Song, Y., and Xie, Y., 2010, Geochronology and geochemisty of the Neoproterozoic granitoid association from eastern segment of the Jiangnan orogen, China Constraints on the timing and process of amalgamation between the Yangtze and Cathaysia blocks: Acta Petrologica Sinica, v. 26, p. 3215–3244. [in Chinese with English abstract.]

Yang, C., Li, X., Wang, X., and Lan, Z., 2015, Mid-Neoproterozoic angular unconformity in the Yangtze Block revisited: Insights from detrital zircon U-Pb age and Hf-O isotopes: Precambrian Research, v. 266, p. 165–178. doi:10.1016/j.precamres.2015.05.016

Yang, Y.-N., Wang, X.-C., Li, Q.-L., and Li, X.-H., 2016, Integrated in situ U–Pb age and Hf–O analyses of zircon from Suixian Group in northern Yangtze: New insights into the Neoproterozoic low-δ 18 O magmas in the South China Block: Precambrian Research, v. 273, p. 151–164. doi:10.1016/j.precamres.2015.12.008

Yao, J., Shu, L., and Santosh, M., 2014a, Neoproterozoic arc–Trench system and breakup of the South China Craton: Constraints from N–MORB type and arc-related mafic rocks, and anorogenic granite in the Jiangnan orogenic belt: Precambrian Research, v. 247, p. 187–207. doi:10.1016/j.precamres.2014.04.008

Yao, J., Shu, L., Santosh, M., and Li, J., 2013, Geochronology and Hf isotope of detrital zircons from Precambrian sequences in the eastern Jiangnan Orogen: Constraining the assembly of Yangtze and Cathaysia Blocks in South China: Journal of Asian Earth Sciences, v. 74, p. 225–243. doi:10.1016/j.jseaes.2012.08.010

Yao, J., Shu, L., Santosh, M., and Li, J., 2015, Neoproterozoic arc-related andesite and orogeny-related unconformity in the eastern Jiangnan orogenic belt: Constraints on the assembly of the Yangtze and Cathaysia blocks in South China: Precambrian Research, v. 262, p. 84–100. doi:10.1016/j.precamres.2015.02.021

Yao, J., Shu, L., Santosh, M., and Zhao, G., 2014b, Neoproterozoic arc-related mafic–Ultramafic rocks and syn-collision granite from the western segment of the Jiangnan Orogen, South China: Constraints on the Neoproterozoic assembly of the Yangtze and Cathaysia Blocks: Precambrian Research, v. 243, p. 39–62. doi:10.1016/j.precamres.2013.12.027

Ye, M., Li, X., Li, W., Liu, Y., and Li, Z., 2007, SHRIMP zircon U–Pb geochronological and whole-rock geochemical evidence for an early Neoproterozoic Sibaoan magmatic arc along the southeastern margin of the Yangtze Block: Gondwana Research, v. 12, p. 144–156. doi:10.1016/j.gr.2006.09.001

Zhang, C., Santosh, M., Zou, H., Li, H., and Huang, W., 2013a, The Fuchuan ophiolite in Jiangnan Orogen: Geochemistry, zircon U–Pb geochronology, Hf isotope and implications for the Neoproterozoic assembly of South China: Lithos, v. 179, p. 263–274. doi:10.1016/j.lithos.2013.08.015

Zhang, S., Wu, R., and Zheng, Y., 2012a, Neoproterozoic continental accretion in South China: Geochemical evidence from the Fuchuan ophiolite in the Jiangnan orogen: Precambrian Research, v. 220–221, p. 45–64. doi:10.1016/j.precamres.2012.07.010

Zhang, Y., Wang, Y., Fan, W., Zhang, A., and Ma, L., 2012b, Geochronological and geochemical constraints on the metasomatised source for the Neoproterozoic (□ 825Ma) high-mg volcanic rocks from the Cangshuipu area (Hunan Province) along the Jiangnan domain and their tectonic implications: Precambrian Research, v. 220–221, p. 139–157. doi:10.1016/j.precamres.2012.07.003

Zhang, Y., Wang, Y., Geng, H., Zhang, Y., Fan, W., and Zhong, H., 2013b, Early Neoproterozoic (□ 850 Ma) back–Arc basin in the Central Jiangnan Orogen (Eastern South China): Geochronological and petrogenetic constraints from meta–Basalts: Precambrian Research, v. 231, p. 325–342. doi:10.1016/j.precamres.2013.03.016

Zhao, G., and Cawood, P.A., 2012, Precambrian geology of China: Precambrian Research, v. 222–223, p. 13–54. doi:10.1016/j.precamres.2012.09.017

Zhao, J., Zhou, M., Yan, D., Zheng, J., and Li, J., 2011, Reappraisal of the ages of Neoproterozoic strata in South China: No connection with the Grenvillian orogeny: Geology, v. 39, p. 299–302. doi:10.1130/G31701.1

Zheng, Y., Gong, B., Zhao, Z., Wu, Y., and Chen, F., 2008b, Zircon U–Pb age and O isotope evidence for Neoproterozoic low-18O magmatism during supercontinental rifting in South China: Implications for the snowball earth event: American Journal of Science, v. 308, p. 484–516. doi:10.2475/04.2008.04

Zheng, Y., Wu, R., Wu, Y., Zhang, S., Yuan, H., and Wu, F., 2008, Rift melting of juvenile arc–Derived crust: Geochemical evidence from Neoproterozoic volcanic and granitic rocks in the Jiangnan Orogen, South China: Precambrian Research, v. 163, p. 351–383. doi:10.1016/j.precamres.2008.01.004

Zhong, Y., Ma, C., Lin, G., and Wang, R., 2005, The SHRIMP U–Pb geochronology of zircons from the composite batholith of Jiulingshan granitoids, Jiangxi Province: Earth Science, v. 30, p. 685–691. [in Chinese with English abstract.]

Zhou, J., Li, X., Ge, W., and Li, Z., 2007a, Age and origin of middle Neoproterozoic mafic magmatism in southern Yangtze Block and relevance to the break–Up of Rodinia: Gondwana Research, v. 12, p. 184–197. doi:10.1016/j.gr.2006.10.011

Zhou, J., Li, X., Ge, W., and Liu, Y., 2007b, Geochronology mantle source and geo–Logical implications of neoproterozoic ultramafic rocks from Yuanbaoshan area of Northern Guangxi: Geological Science and Technology Information, v. 26, p. 11–18. [in Chinese with English abstract.]

Zhou, J., Wang, X., and Qiu, J., 2009, Geochronology of Neoproterozoic mafic rocks and sandstones from northeastern Guizhou, South China: Coeval arc magmatism and sedimentation: Precambrian Research, v. 170, p. 27–42. doi:10.1016/j.precamres.2008.11.002

Zhou, M., Yan, D., Kennedy, A.K., Li, Y., and Ding, J., 2002, SHRIMP U–Pb zircon geochronological and geochemical evidence for Neoproterozoic arc-magmatism along the western margin of the Yangtze Block, South China: Earth and Planetary Science Letters, v. 196, p. 51–67. doi:10.1016/S0012-821X(01)00595-7

Zhou, X., Zou, H., Yang, J., and Wang, Y., 1990, Sm–Nd isochronous age of Fuchuan ophiolite suite in Shexian county, Anhui Province and its geological significance: Chinese Science Bulletin, v. 35, p. 208–212.